Chem Soc Rev

REVIEW ARTICLE

View Article Online
View Journal

Cite this: DOI: 10.1039/d5cs01553g

Direct impure water electrolysis at industrial scale

Jichao Zhang,[a] Jianrui Feng,[b] Daojin Zhou, *[c] Hongtao Wang,*[a] Wei Liu,[d] Longxiang Liu,[e] Wei Zong, [f] Jiexin Zhu,[g] Ruwei Chen,[b] Hongzhen He,[h] Mingqiang Liu,[i] Wei Zhang,[j] Faze Chen, *[k] Ivan P. Parkin, [b] Xiaoming Sun *[c] and Guanjie He *[b]

Received 17th March 2026

DOI: 10.1039/d5cs01553g

rsc.li/chem-soc-rev

Without reliance on freshwater, direct impure water electrolysis (DIWE) enriches the vision of sustainably producing green hydrogen in regions with a geographical mismatch between freshwater and renewable resources. However, the roadmap of industrialization is fraught with a pyramid of interconnected challenges, especially stemming from performance degradation. Herein, this review provides a timely appraisal of diverse impurities present in seawater and wastewater. The specific impacts of impurities were reassessed to highlight the synergistic optimization toward industrial-scale implementation. Moreover, we pioneered a lucid industrial pathway based on the impurity-induced interplay. The technical and economic viability of integrating the DIWE process into existing industrial workflows was emphasized to outline promising avenues for future research.

1. Introduction

A rapid transition from fossil fuels to renewable electricity holds promise for global decarbonization.[1–3] However, particularly in aviation and shipping, carbon emissions cannot be effectively alleviated by electrification alone.[4–9] Hydrogen (H_2), a feedstock for fertilizer production and oil refining, has been extensively explored as a complementary candidate for

[a] SINOPEC (Dalian) Research Institute of Petroleum and Petrochemicals Co., Ltd, Dalian, Liaoning 116045, China. E-mail: wanghongtao.fshy@sinopec.com
[b] Christopher Ingold Laboratory, Department of Chemistry, University College London (UCL), 20 Gordon Street, London WC1H 0AJ, UK. E-mail: g.he@ucl.ac.uk
[c] State Key Laboratory of Chemical Resource Engineering, College of Chemistry, Beijing University of Chemical Technology, Beijing, P. R. China. E-mail: zhoudj@buct.edu.cn, sunxm@mail.buct.edu.cn
[d] Department of Chemistry, Northwestern University, Evanston, IL 60208, USA
[e] Department of Materials, University of Oxford, Parks Road, Oxford, OX1 3PH, UK
[f] Department of Engineering Science, University of Oxford, Parks Road, Oxford OX1 3PJ, UK
[g] Department of Mechanical and Industrial Engineering, University of Toronto, Toronto, ON M5S 3G8, Canada
[h] Department of Earth Science and Engineering, Imperial College London, London, SW7 2AZ, UK
[i] Max Planck Institute for Sustainable Materials, Max-Planck-Straße 1, 40237 Düsseldorf, Germany
[j] Department of Chemical and NanoEngineering, University of California San Diego, La Jolla, CA, USA
[k] School of Mechanical Engineering, Tianjin University, Tianjin 300350, China. E-mail: faze.chen@tju.edu.cn

Jichao Zhang

Dr Jichao Zhang was awarded a PhD degree in 2024 from Prof. Ivan P. Parkin and Prof. Guanjie He's group at UCL Chemistry. He is currently working at SINOPEC and focuses on the design of novel electrocatalysts and devices for impure water electrolysis towards industrial applications. His group has been leading China's first factory-based seawater hydrogen production project.

Jianrui Feng

Mr Jianrui Feng was awarded a B.S degree in 2016 from Nankai University. He is currently working as a PhD candidate in Prof. Ivan P. Parkin and Prof. Guanjie He's group at UCL Chemistry. He focuses on theoretical computations and operando experiments to reveal the structure-performance relationship for impure water electrolysis and energy storage systems.

bolstering energy security in the near-term future.[10–13] The world's major economies (the USA, China, the EU, and Japan) have published their national strategies.[14] International H_2 supply chains are projected to be established with at least 148 Mt per year by 2050.[15–17] Unfortunately, conventional industrial-scale grey and blue H_2 production has adverse environmental effects.[18–20] The widely-used approaches, such as coal gasification ($2C + O_2 + 2H_2O \rightarrow 2H_2 + 2CO_2$) and steam methane reforming ($CH_4 + 2H_2O \rightarrow 4H_2 + CO_2$), inevitably incorporate consequential carbon emissions.[21–24]

As an environmentally-friendly method to sustainably produce H_2, renewable-electricity-powered water electrolysis ($2H_2O \rightarrow 2H_2 + O_2$) has gained more attention due to the availability of ample renewables (*e.g.*, wind and solar power).[25–28] As shown in Fig. 1, this promising approach revolutionizes the usage of green H_2 in extensive scenarios, involving metallurgy in the steel industry, alternative fuel in cement production, chemicals production, long-duration energy storage, personal vehicles, heavy-duty and long-haul transport.[29–35] Nonetheless, commercial high-purity water electrolysis (HPWE), such as proton exchange membrane (PEM)-based and alkaline (ALK)-based systems, necessitates a freshwater-intensive supply to meet the conductivity threshold below 1 mS m^{-1} for ALK systems and an even lower threshold of 0.1 mS m^{-1} for PEM systems.[36–40] The readily accessible freshwater accounts for only 0.01% of the global water resources.[41] It is estimated to consume ~3.7 Mt of freshwater per day to achieve the goal of a minimum of 148 Mt H_2 per year, exacerbating the shortage of global freshwater resources.[42] Notably, a geographical mismatch exists between renewable energy and freshwater resources.[43–47] China serves as a key example, where major wind and solar resources are located in freshwater-scarce eastern offshore and inland arid regions.[44] Similarly, worldwide regions, such as North Africa and the Middle East, also exhibit resource mismatches: rich renewable sources but limited freshwater.[48–51] Therefore, this issue has sparked extensive research interest in the exploration of alternative feedwater sources.

Impure water electrolysis (IWE) is one of the most promising strategies to ameliorate reliance on ultrapure water.[52] Seawater,

Daojin Zhou

Dr Daojin Zhou was awarded a PhD degree in 2019 from Beijing University of Chemical Technology and currently works as an associate professor. His recent work focuses on the design of novel electrocatalysts and devices for impure water electrolysis. He has published multiple high-quality papers in the leading chemistry, materials, and energy journals.

Ivan P. Parkin

Prof. Ivan P. Parkin, ranked within the world's top 500 scientists by subject area (materials science based on citations in the previous ten years), is the Dean of Mathematical and Physical Sciences at UCL. He has supervised over 150 PhD students in his 30-year career at UCL. He has been awarded 9 Prizes and medals and is a fellow of the Royal Society of Chemistry and a member of the Academia European. He has co-authored over 1000 scientific papers with citations over 70 000 and an H-index of 128. His group works on energy conversion and storage applications based on electrochemistry.

Xiaoming Sun

Prof. Xiaoming Sun joined the State Key Laboratory of Chemical Resource Engineering, Beijing University of Chemical Technology, in 2008. His recent work focuses on impure water electrolysis. Prof. Xiaoming Sun has co-authored over 200 scientific papers with citations over 80 000.

Guanjie He

Prof. Guanjie He is a Professor in Materials Chemistry and Engineering, and an ERC Starting Grant Awardee at University College London (UCL). He is an elected Fellow of the Royal Society of Chemistry (FRSC) and a Fellow of the Institute of Materials, Minerals and Mining (FIMMM). His recent work focuses on aqueous energy storage and conversion materials and devices, advanced characterization, and AI for chemistry and electrochemical engineering.

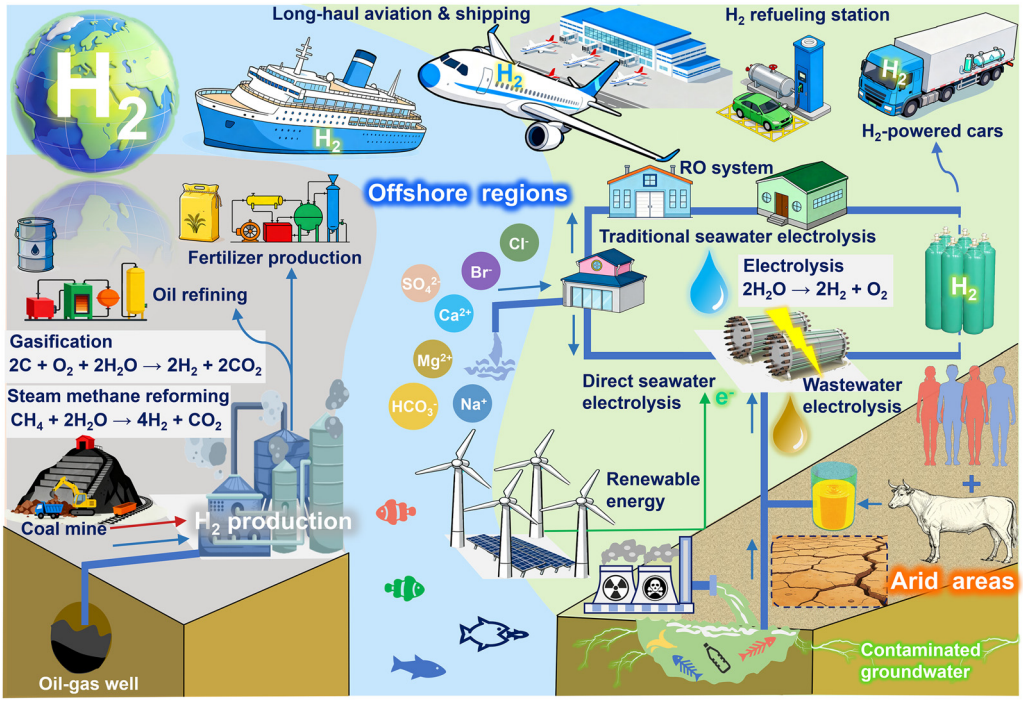

Fig. 1 Schematic illustrations of the production and utilization of H_2 in practical scenarios. H_2 plays a crucial role in achieving a carbon-neutral society. As compared to grey and blue H_2, green H_2 produced by renewable energy is anticipated to be applied for industry and transportation in a more environmentally friendly way. In this context, direct impure water electrolysis, such as electrolysis of seawater and wastewater, holds great potential to circumvent the use of high-purity feedwater in offshore and arid areas.

accounting for 96.5% of water reserves, implies an almost infinite water resource.[53] The abundant natural seawater could be exploited in offshore platforms for H_2 production, reducing both operational expenditure (OPEX) and capital expenditures (CAPEX) of seawater desalination.[54] When deeply integrated into offshore-generated renewable power, H_2 produced from seawater electrolysis further plays a crucial role as a dispatchable energy storage to surmount the intermittency of renewable power, minimizing grid losses and enhancing energy efficiency.[55–58] Conversely, natural water reserves are limited in many inland arid areas. Against this background, the high-efficiency recycling of limited water sources is indispensable.[59] In particular, diverse wastewater represents over 50% of total freshwater withdrawals.[60–62] However, it is reported that only 11% of wastewater worldwide is recycled.[63] Nearly half of untreated industrial, agricultural, and domestic wastewater still ends up in natural water bodies, resulting in groundwater contamination.[64] Consequently, should we rationally valorize wastewater to produce green H_2 and high-value-added by-products, a win-win synergy between water remediation and a sustainable hydrogen economy will be realized.[65]

Despite the encouraging prospect of the IWE-based technical route, there is a large gap from lab to market.[66] Compared to HPWE, IWE faces more formidable challenges in dealing with water impurities.[67] Crucially, both seawater and wastewater contain a wide variety of ions.[68] For instance, anions and cations, including halide ions (*e.g.*, Br^-, Cl^-) and metal ions (*e.g.*, Ca^{2+}, Mg^{2+}), are known to undergo side reactions and form inorganic precipitates, compromising operational lifespan.[69] Analogously, other impurities, including organic compounds,[70–73] microscopic organisms,[74] dissolved gases,[75] microplastics,[76] *etc.*, can potentially provoke unwanted impacts. Concomitantly, *in situ*-generated impurities derived from the dissolution of metal-based device components carry the risk of impairing system performance.[77] Furthermore, various undesired gaseous by-products can contaminate H_2, leading to additional gas purification.[78–80] Aside from these inherent challenges, the reliability of indirect IWE remains subject to debate. The reverse-osmosis (RO) system has been widely employed for desalination to achieve a lower concentration of ionic impurities than that of seawater.[81] Qiao's group proposed a two-complementary-protection strategy for stable electrolysis of RO water in the PEM system.[82] However, when the water purification system goes down, elevated impurity levels in feedwater can inevitably elicit serious performance deterioration.[83] Therefore, additional purification steps, with the incremental cost of installation and maintenance, raise the question of whether the indirect IWE meets the requirements for large-scale industrial applications.

Obviously, removing all impurities to obtain ultrapure water going into the electrolyzer remains impractical. Metal catalysts are prone to deactivation due to metal leaching into the electrolyte during long-term operation, compromising the original purity of the feedwater in the HPWE system.[84–86] Due to the difficulty of maintaining the high-purity of the feedwater, developing direct impure water electrolysis (DIWE) is thereby

proposed to reduce costs, simplify processes, and provide meaningful guidance for HPWE-related research. Despite some debates about the negligible cost reduction, it is crucial to clarify that the development trajectory of DIWE should not be limited to obtaining cheaper H_2. Moreover, the high tolerance to varying water qualities undoubtedly broadens the application scope. Ling's group consecutively claimed a series of strategies towards highly efficient direct seawater electrolysis (DSE) and the PEM system with cationic impurities.[87–89] Regrettably, the current studies on impurity-induced degradation mechanisms, cost-effective catalysts, durable electrolyzers, and process integration are still in their infancy.[90] As shown in Fig. 2 and the comparison table (Fig. S1, SI), most reviews are either too outdated to reflect the recent progress or partially focus on performance enhancement with a lab mindset.[91–94] Consequently, a broader consensus on the role that DIWE will play within the future landscape of the H_2 economy should be reached.[95–97]

Based on the aforementioned discussion, we first analyzed the advantages of DIWE among mainstream technologies and corresponding impurity-induced challenges in this timely review. Subsequently, to tackle the above challenges, the advances in the development of scenario-oriented electrocatalysts and function-oriented electrolyzers were summarized. Lastly, underpinned by impurity-induced interaction mechanisms, we pioneered the collaborative optimization of device components to integrate DIWE technology into existing industrial workflows. The future outlook further paves the way for the goal of fully realizing the industrial application.

2. Importance of using impure water

As warned by the latest report from the United Nations research agency, our planet is entering an era of global "water bankruptcy".[98] Long-term water consumption has not only outstripped the water renewal capacity of the planet, but may have also crossed an irreversible threshold. With the development of green H_2, a large amount of high-purity water is consumed, aggravating the water scarcity, especially in areas with uneven freshwater distribution. As for offshore and inland arid regions with ample solar and wind resources, impure water has been a promising candidate for sustainably producing H_2, such as natural seawater and wastewater. In this section, a comprehensive analysis of the advantages of DIWE technology over other mainstream technologies was conducted. A systematic comparison was subsequently performed in terms of techno-

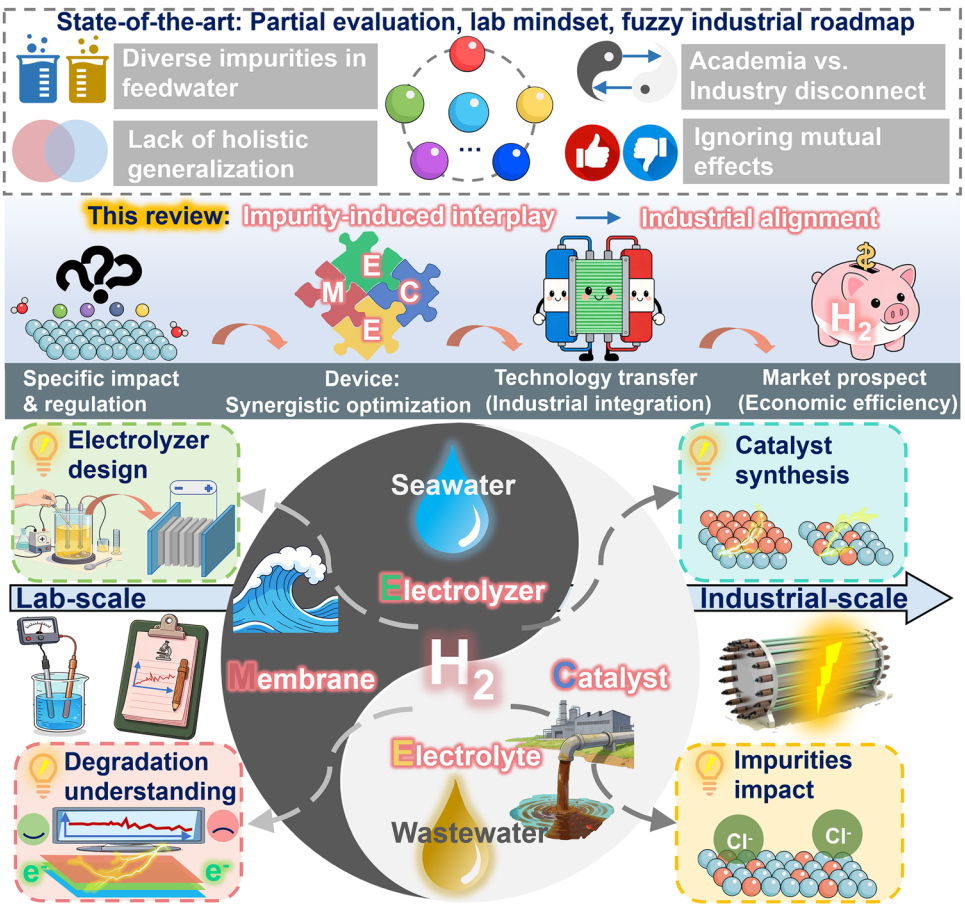

Fig. 2 Schematic summary of the impurity-induced interplay for impure water electrolysis at industrial scale. As compared to other review papers, we provided a comprehensive summary of impurity-induced interplay. The gap between the lab and industry was also bridged. Synergistic optimization for realizing full-chain improvement in real-world conditions was highlighted.

economic and environmental impact. Based on our academic and industry experience, the potential impurity-induced challenges were ultimately introduced.

2.1. Advantages of DIWE technology

The pivotal role of green H_2 has attracted widespread attention from global energy suppliers. However, the production costs pose a major hurdle to developing the H_2 economy. In the current HPWE process, high-quality feedwater is usually required to ensure the lifespan of the H_2 plant infrastructure. Expensive deionization processes are commonly carried out to remove undesired ions to maintain a conductivity threshold.[99–102] More importantly, the *in situ*-generated impurities during the HPWE process could also compromise the high purity of feedwater. Accordingly, from the perspective of techno-economic feasibility and environmental impact, the advantages of developing DIWE technology were demonstrated.

2.1.1. Techno-economic feasibility. As shown in Fig. 3, offshore and inland arid regions possess ample renewables but limited freshwater. To leverage renewable power in freshwater-rich regions, long-distance power transmission will potentially cause grid losses. Provided that we select commercial HPWE technologies for on-site production, freshwater transport will be ineluctably needed for preparing electrolytes. Due to the increased production costs of green H_2, the above plans are unfavorable towards industrial-scale implementation. Indirect IWE technology, such as the RO system for desalination, is considered a viable route to employ the local impure water sources. Specifically, Md Golam Kibria's group comprehensively analyzed the seawater RO technology coupled with PEM system (SWRO-PEM), including the daily energy requirement, direct capital cost, operating costs, and levelized cost of H_2.[103] 0.1% of total energy, ~3% of total direct CAPEX, ~0.2% of the total OPEX, and 0.6% of the cost of H_2 are needed by SWRO (Fig. S2, SI). The levelized cost of H_2 reached ~US$3.83 kg^{-1}, predominantly governed by electricity consumption (79.6%). Lei *et al.* further conducted a techno-economic assessment of the offshore H_2 production cost for ALK and PEM system (Fig. S3, SI), including electricity, seawater desalination, replacement, operation and maintenance (O&M) capital costs, and offshore platform building.[104] Analogously, electricity expenditure constitutes the predominant proportion of H_2 production costs, which is 70.5% (ALK) and 57.6% (PEM). The offshore H_2 production costs were calculated to be ~US$3.64 kg^{-1} (ALK) and ~US$4.13 kg^{-1} (PEM). Despite the reduced electricity consumption of the PEM system, higher costs of capital investments, O&M, and desalination than those of the ALK system collectively raise offshore H_2 production expenses.

Notably, the ionic impurity level of RO water, involving cations (*e.g.*, Na^+, Ca^{2+}, and Mg^{2+}) and anions (*e.g.*, Cl^-, F^-, and NO_3^-), is considerably lower than that in natural seawater. Nevertheless, even trace ionic impurities can cause severe degradation of the PEM-based system, especially at high potentials.[82] The installation costs and operational complexity of the further deionization process can remarkably limit the development of indirect IWE.[105–107] Given the complexity of real-world conditions, a continuous supply of ultrapure water into the electrolyzer can hardly be sustained. The failure of additional purification and deionization processes can lead to

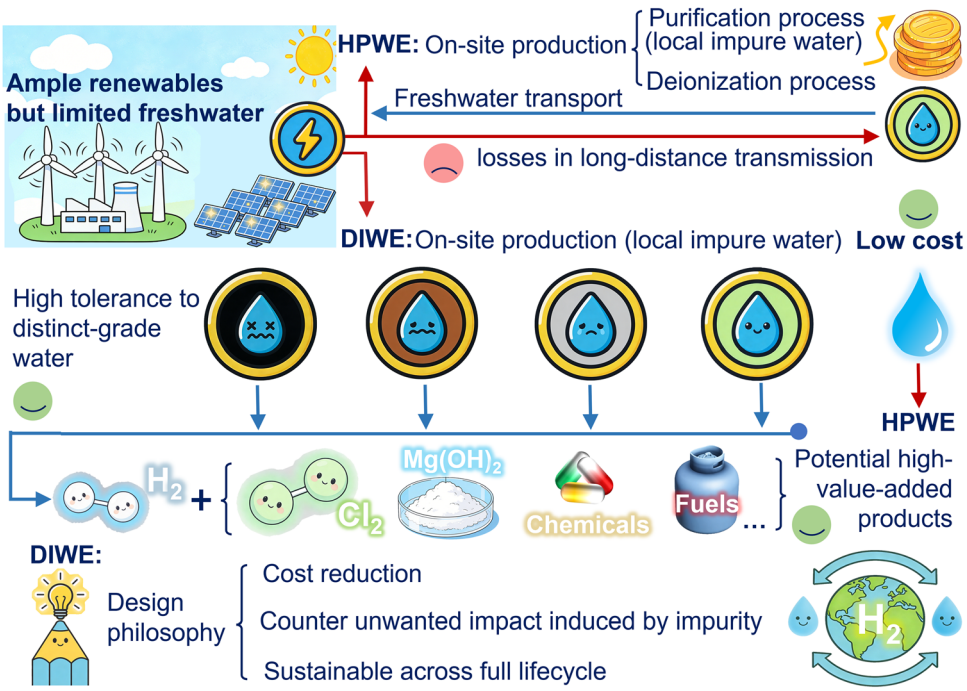

Fig. 3 Schematic summary of the advantages of DIWE technology. Compared with mature technologies, including SWRO-PEM and ALK, this review analyzed the strengths of DIWE in techno-economic viability and environmental effects, verifying the necessity of promoting DIWE technology.

elevated impurity levels, compromising the long-term operation durability. Accordingly, the DIWE technology that directly leverages local impure water showcases a promising route for H_2 production with a streamlined process flow. Concomitantly, tolerance to different grades of feedwater is enhanced by developing suitable device components. As compared to the HPWE system with only H_2 and O_2 as final products, a wide range of impurities is poised to produce high-value-added by-products to boost economic efficiency. Furthermore, developing DIWE technology is expected to inspire the HPWE-related studies to overcome durability issues induced by *in situ*-generated impurities around the reaction microenvironment.

Admittedly, owing to the failure of rapid translation into commercial benefits, the DIWE sparked intense debate.[108] Critics contend that removing the purification step brings about insignificant cost savings. Sustaining long-term durability toward complicated impurities gives rise to additional costs. Fortunately, their concerns have gradually been allayed by the technological breakthroughs in this field. Recent studies on DIWE have verified that the H_2 production cost could be reduced to the 2030 target of \$1 kg^{-1} (Table S1, SI) stipulated by the U.S. Hydrogen Shot programme.[14] For example, Tang's group developed a microscopic bubble/precipitate traffic system that sustained over 150 h at 500 mA cm^{-2} in natural seawater, with an estimated H_2 production cost of US\$1.8 kg^{-1}.[109] Sun's group further proposed a hexafluorophosphate additive strategy, achieving stable operation over 1000 h at 1.0 A cm^{-2}.[110] The H_2 production cost was calculated to be approximately US\$1.07 kg^{-1}. More encouragingly, Lu's group has achieved the simultaneous production of H_2 and high-purity $Mg(OH)_2$ from seawater over 1000 h. This co-production electrolysis system reduced the cost to US\$0.61 kg^{-1}, far below the 2030 target.[111] Over the past four years, sustained research advances have greatly promoted the industrial application. Stable operation for 10 000 hours can be realized simply *via* catalyst modification of non-noble metal materials in mature membrane electrolyzers. This strategy does not significantly raise the energy expenditure arising from impurity interference, catalyst degradation, and maintenance.[112] Phase-transition strategy further enables a H_2 production scale of 1.2 Nm^3 h^{-1} in a real ocean fluctuation environment.[113] In particular, China is projected to reach a cumulative installed capacity of 1880 GW for solar power and 766 GW for wind power, yielding $\sim$4.9 PWh per year by 2030.[114] Due to the dominant proportion of electricity costs, directly integrating low-cost renewable electricity with locally available impure water sources will emerge as one of the mainstream approaches for industrial-scale H_2 production in the near future.

Overall, cost reduction lays a solid foundation for the commercialization of DIWE technology. In this context, six strategies, including plant siting, scaling up, operational optimization, efficiency enhancement, technological advancements, and digital empowerment, are summarized for further cost reduction (Fig. S4, SI). Priority should be given to the rational siting of H_2 production plants. Locating facilities in regions with low electricity prices and abundant water sources could substantially reduce the total cost. Large-scale deployment of electrolyzers, prolonged operating hours, improved operational efficiency, and technological breakthroughs will collectively drive down the total costs. More notably, the adoption of digital technologies can effectively curtail operation and maintenance expenses.

2.1.2. Environmental impact. Beyond the techno-economic viability, the benefits in terms of environmental sustainability are equally remarkable. The environmental impact of HPWE is easily ignored by research communities. Specifically, the acidic or alkaline electrolytes over long-term operation can potentially deviate from their original purity level.[115–117] The post-treatment of used electrolytes should be carefully performed to prevent direct discharge from damaging the ecosystem. More importantly, in the indirect IWE system, disposal of brine generated by the desalination process can potentially jeopardize the local ecosystem.[118] Instead, as a more promising alternative to HPWE and indirect IWE, DIWE offers a more sustainable and flexible solution. In addition to reducing the H_2 production costs, the design philosophy of DIWE technology is also based on counteracting the impact of impurities and delivering the circular concept across the full lifecycle. Distinct-grade impure water is expected to be treated in specific scenarios based on the DIWE technology. Notably, the aforementioned acidic or alkaline waste electrolyte from the HPWE system can be repurposed by utilizing robust catalysts and impurity-resistant electrolyzers. Besides, every city has its own wastewater treatment plant, where the reclaimed water can be directly electrolyzed by simply acidifying wastewater effluent to suppress the negative impact of cationic impurities.[119] With relatively well-defined impurities, abundant natural seawater also holds potential to be leveraged in the anti-corrosion electrolysis system.[120] Therefore, the environmentally benign principle of advancing water recycling represents another competitive advantage of DIWE technology.

2.2. Impurity-induced challenges

Despite the advantages of DIWE technology, the specific impact of impurities remains ambiguous. In this section, the main impacts and potential challenges incurred by a wide range of complicated impurities were first summarized in terms of catalysts and relevant electrolyzer components. The system fluctuation was subsequently considered to reveal the interfacial dynamic evolution. The most harmful impurities for both seawater electrolysis and wastewater electrolysis were summarized in the comparison table (Fig. S5, SI), demonstrating where the field still disagrees and pointing out the biggest knowledge gaps. The potential bottleneck issues in this section, such as electrode corrosion and electrolyzer failure, were comprehensively analysed, paving the way for the following discussion of the synergistic optimization.

2.2.1. Cations. Cations are one of the most common impurities in both seawater and wastewater. Take seawater as an example, sodium (Na^+) accounts for 30.59% of the major components, followed by magnesium (Mg^{2+}, 3.68%), calcium (Ca^{2+}, 1.18%), and potassium (K^+, 1.11%).[121] Similarly, those cations could also be detected in diverse wastewater from industrial,

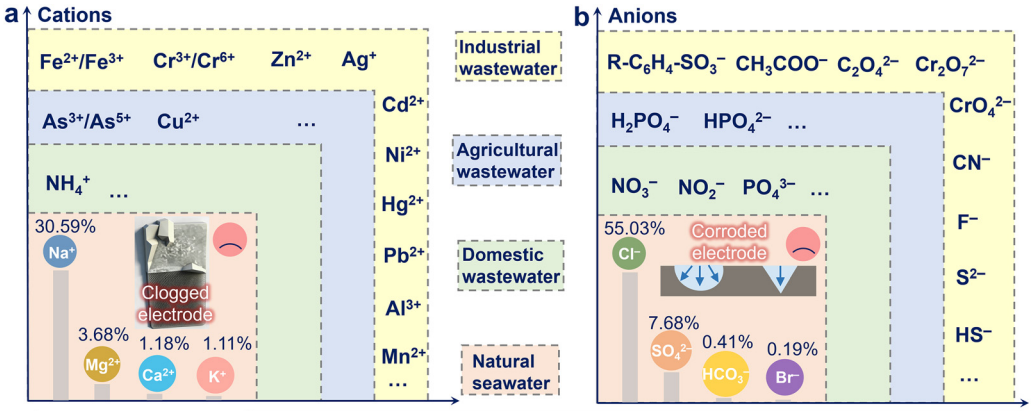

c

Ionic impurities	Main impact and potential challenges
Na^+ K^+ Li^+	Selectivity: Regulate diffusion barrier Lacking spectroscopic verification generalization Catalyst: Enhance activity of layered catalysts Membrane: Conductivity loss
Ca^{2+} Mg^{2+} NH_4^+	Catalyst: Deactivation by hydroxide precipitates EDL: Boost the connectivity of H-bonded networks Inhibit precipitates formation Membrane: Conductivity loss
Cu^{2+} Ag^+ Fe^{2+}/Fe^{3+}	Catalyst: Deactivation by undesired deposition Catalyst: Enhance activity and stability of earth-abundant catalysts Under-researched understanding of dissolution–re-adsorption Membrane: Fenton reaction induced degradation
Cl^- Br^-	Catalyst: Side-reaction; corrosion Membrane: Affect Ion conductivity and durability
SO_4^{2-} PO_4^{3-} F^- HCO_3^-/CO_3^{2-}	EDL: Repel Cl^- adsorption Reasonable hypothesis rather than confirmed mechanism Catalyst: Specific adsorption of SO_4^{2-} on noble metal TBL/BPP: F^- induced Ti corrosion
$C_2O_4^{2-}$ $R\text{-}C_6H_4\text{-}SO_3^-$	Under-researched mechanism

Fig. 4 Summary of the representative ionic impurities and impurity-induced challenges. (a) and (b) Common cationic and anionic impurities in natural seawater and various wastewater from domestic, agricultural, and industrial sources. (c) The list of representative ionic impurities and their main impacts and potential challenges toward the electrolysis system was presented. We comprehensively summarized the positive and negative roles of some ionic impurities, as well as the under-researched mechanism.

agricultural, and domestic areas, as shown in Fig. 4a. Moreover, ammonium (NH_4^+), a product from the hydrolysis of urea in human and animal excreta, is the main form of nitrogen from sources such as fertilizer manufacturing, domestic sewage, livestock, and poultry farming.[122–126] Furthermore, some metal cations, such as copper (Cu^{2+}), iron (Fe^{2+}/Fe^{3+}) and silver (Ag^+), originate from agricultural and industrial wastewater, involving pesticides, electroplating, metallurgy, tanning, electrical soldering, battery manufacturing, pigment production, *etc.*[127–131] Notably, heavy metal cations, with strong biological toxicity, are detrimental to human beings, potentially causing accumulation in the biological chain.[132]

The impact and persistent challenges provoked by specific cationic impurities were subsequently revealed in practical scenarios. Abundant alkali metal cations in natural seawater, such as Na^+ ($\sim$0.47 mol L^{-1}) and K^+ ($\sim$0.01 mol L^{-1}), can serve as raw materials for chemical synthesis. Seawater also contains a low concentration of lithium (Li^+, $\sim$0.0025 mol L^{-1}) that possesses high economic value for the battery industry. Nakamura's group has recently demonstrated that alkali cations could regulate chloride diffusion, resulting in a significant improvement in the selectivity of the water oxidation reaction.[133] Li^+ possessed the strongest diffusion barrier among the other examined cations (*e.g.*, Na^+ and K^+), implying that the selectivity could be increased in the presence of Li^+. However, further spectroscopic verification and generalization are lacking to strategically leverage certain ionic imuprities for enhanced electrocatalytic processes. Additionally, Boettcher's group claimed that electrolytes containing the alkali metal cations (Na^+ and K^+) yielded dramatically lower overpotentials in alkaline media.[134] When penetrating the layered structure of Ni–Fe oxyhydroxide in alkaline media, Na^+ and K^+, with an optimal acidity and size,

ensured not to bind too strongly or to alter the stability of reaction intermediates. Nonetheless, most cationic ions (*e.g.*, Na^+, K^+, Ca^{2+}, *etc.*) can potentially disrupt proton transport and reduce electrochemical reaction rates in PEM-based electrolyzers.[52]

As compared to alkali metal cations, Mg^{2+} ($\sim$0.053 mol L^{-1}) and Ca^{2+} ($\sim$0.01 mol L^{-1}) are also rich in natural seawater. They are indispensable to pharmaceuticals, food additives, paper, plastics, and the construction industry. However, during the hydrogen evolution reaction (HER) process, the local pH value can increase significantly due to the rapid consumption of protons. Mg^{2+} and Ca^{2+} are susceptible to reacting with hydroxide ions (OH^-) to form the insoluble metal hydroxides on the cathode surface. These precipitates are non-conductive, thereby triggering the blockage of active sites to inhibit HER.[135–138] Although acidic conditions can effectively suppress the formation of metal hydroxides, a striking fluctuation of local basic pH values ($\geq\sim$9.5) will potentially lead to undesirable hydroxide precipitation.[109,139–141] Recently, Gao's group reported that NH_4^+ could be hydrogen-bonded with OH^- from the interfacial H_2O dissociation and thereby inhibited the formation of hydroxide precipitates.[142] Meanwhile, these NH_4^+ groups were able to boost the connectivity of hydrogen-bonded networks in the electric double layer (EDL), lowering the proton transfer barrier and improving the HER energetics. Regrettably, increased concentration of such non-metallic cations can also undermine the membrane conductivity.[143–145]

In addition, some reducible cation contaminants with sufficiently positive standard electrode potential, such as Ag^+ and Cu^{2+} in tap water, are prone to being deposited during the HER process, inducing unwanted activity degradation.[100] More intriguingly, the dynamic role of cationic Fe impurities has attracted extensive attention. Boettcher's group found that the introduction of Fe into the Ni-based hydroxides could incur a variation in the activity of the oxygen evolution reaction (OER).[146] Besides, Mullins's group also discovered that Fe impurities served as a conducive factor to enhance the OER activity when tested in Fe-unpurified alkaline electrolytes.[147] Besides, the adverse effect of Fe impurities cannot be overlooked. Fe^{2+}, possibly leaching from stainless steel bipolar plate corrosion, would initiate Fenton reactions, producing hydroxyl radicals that degrade the perfluorosulfonic acid (PFSA) backbone of the membrane.[148] Analogously, cationic impurities in industrial wastewater, such as chromium (Cr^{3+}/Cr^{6+}), lead (Pb^{2+}), cadmium (Cd^{2+}), *etc.*, can also adversely affect electrolyzer components, posing tremendous challenges in further developing DIWE technology.

2.2.2. Anions. Anions exert an equally critical influence on catalysts as well as relevant electrolyzer components. Chloride (Cl^-) accounts for 55.03% of the major ion composition of seawater, which is followed by sulfate (SO_4^{2-}, 7.68%), bicarbonate (HCO_3^-, 0.41%), and bromide (Br^-, 0.19%).[121] Those anions could also be discerned in various wastewater sources from industrial, agricultural, and domestic areas, as shown in Fig. 4b. Also, nitrate (NO_3^-) and nitrite (NO_2^-) are considered as the main anionic components from the nitrification of NH_4^+.[149] Phosphate (PO_4^{3-}) is easily detected in phosphorus-containing detergents and human excrement.[150–153] Furthermore, other anions, such as dihydrogen/monohydrogen phosphate ($H_2PO_4^-$/HPO_4^{2-}), chromate/dichromate (CrO_4^{2-}/$Cr_2O_7^{2-}$), fluoride (F^-), sulfide/bisulfide (S^{2-}/HS^-), oxalate ($C_2O_4^{2-}$), acetate (CH_3COO^-), alkylbenzenesulfonate (R–C_6H_4–SO_3^-), *etc.*, are easily detected in agricultural and industrial wastewater, involving phosphate fertilizers, electroplating, semiconductors, fluorine chemicals, petroleum refining, food processing, and the cleaning industry, *etc.*[154–157]

The main impacts and persistent challenges engendered by specific anionic impurities were subsequently revealed in practical scenarios. Cl^- is an abundant anion in natural seawater ($\sim$0.55 mol L^{-1}) and wastewater.[69] As a formidable challenge, the electro-oxidation reaction of Cl^- (ClOR), a rapid two-electron transfer process, can kinetically outcompete inherently sluggish four-electron OER in acidic electrolytes.[158] Conversely, the OER is thermodynamically more favorable than the ClOR in alkaline media, with a potential difference of 0.48 V. Nonetheless, achieving the amper-level current density with a lower overpotential is considered a challenging task.[66] The generation of corrosive species, including hypochlorite (ClO^-) species in alkaline medium and chlorine (Cl_2) in acidic medium, further elicits electrode degradation and breakdown of electrolyzer components, diminishing electrolysis efficiency and durability.[100] Furthermore, the electrode corroded by a low concentration of Br^- ($\sim$0.00084 mol L^{-1}) in natural seawater is easily overlooked. Lu's group ascertained that Br^- poses a greater threats to non-noble-metal anodes.[159] Due to the faster corrosion kinetics, extensive etching of Br^- resulted in shallow-wide pits, as compared to narrow-deep pits by local Cl^- corrosion. More detrimentally, halides (*e.g.*, Cl^- and Br^-) and their derivatives can also compromise the properties of membranes (ionic conductivity and durability).[160]

Oxyanion impurities, such as sulfate (SO_4^{2-}, $\sim$0.028 mol L^{-1}) and bicarbonate or carbonate (HCO_3^-/CO_3^{2-}, $\sim$0.002 mol L^{-1}) in natural seawater, have been regarded as positive additives for enhancing durability. Chen's group affirmed that remarkable improvement of stability was achieved by adding SO_4^{2-}. The preferential adsorption of the SO_4^{2-} repulsed Cl^- attack by the electrostatic repulsive forces.[161] However, specific adsorption of SO_4^{2-} on noble metal catalysts can potentially shift the onset with undesired performance degradation.[162–164] The intercalation of other anionic impurities into layered catalysts, such as HCO_3^-/CO_3^{2-}, and PO_4^{3-}, has been evidenced as another effective strategy to suppress Cl^- adsorption.[165–169] F^-, at a low concentration of ($\sim$0.00007 mol L^{-1}) in natural seawater, possesses high electronegativity.[69] Utilizing this unique property was proven to be an efficient strategy for tailoring the OER selectivity. The introduction of F^- was verified to boost the free water content and regulate the hydrogen bond network with favorable OH^- transportation.[170] Despite its widespread adoption as an ion-repelling strategy, this method remains subject to debate over plausible hypotheses instead of confirmed mechanisms. Sufficient direct evidence from both

operando experiments and theoretical calculations has rarely been reported to reveal the dynamic variation of surface charges around the reaction microenvironment. More adversely, as crucial electrolyzer components in the PEM-based system, the porous transport layer and bipolar plate (PTL/BPP) are usually made of titanium (Ti)-based materials. F^- was evidenced to corrode the titanium oxide (TiO_2) passive film (corrosion protective layer), with a threshold corrosion concentration of 0.0005–0.02 mol L^{-1} F^- in 0.05 M H_2SO_4 and 0.001 mol L^{-1} F^- in 1 M $HClO_4$.[171–174]

Organic anionic impurities, with negatively charged organic molecules, are commonly distributed in various industrial and municipal wastewater. For example, $C_2O_4^{2-}$, regarded as a chelating agent and pH regulator, is widely used in the textile and leather industries.[175] Tang's group reported an *in situ* self-transformation tactic, converting $C_2O_4^{2-}$ to CO_3^{2-} for suppressing the unwanted ClOR.[140] Besides, surfactants pollute water during household and industrial washing processes. Linear alkyl benzene sulfonate (LAS, R–C_6H_4–SO_3^-), characterized by a hydrophobic 'tail' and a hydrophilic 'head', is the largest group of anionic surfactants in detergents, with a concentration of 3–21 mg L^{-1} in domestic sewage.[176] Our group has carried out a performance test in alkaline domestic dishwashing wastewater to corroborate the applicability of non-noble metal catalysts.[177] Despite the outstanding activity and stability of the as-prepared catalysts, the specific impact of the organic anions remains ambiguous due to their complicated physicochemical properties.

Consequently, the main impacts and potential challenges of the above-mentioned cationic and anionic impurities are outlined in Fig. 4c. Despite the partial summarization, it is impractical to include all the ionic impurities owing to the complexity and diversity of impure water sources. The introduction of representative ionic impurities and their specific impact has systematically pointed out the most common impurity-induced challenges, paving the way for the subsequent development of catalysts and relevant electrolyzer components. More crucially, it is advisable to comprehensively evaluate both favorable and adverse impacts of impurities across the entire system.

2.2.3. Non-ionic impurities. Impurities are generally classified into two different types: exogenous and endogenous impurities.[52] Exogenous impurities are identified as those originally contained in distinct-grade water. Apart from the above-mentioned ionic impurities, organic impurities, mainly from conventional organic wastewater, biomass wastewater, and nitrogenous wastewater, are able to exert impending threats to the system performance.[178] As shown in Fig. 5, those small molecules, with a lower thermodynamic potential than that of the OER, are preferentially oxidized at the anode, reducing the voltage required to obtain the same current density. However, the products, carbon monoxide (CO) and carbon dioxide (CO_2), can potentially poison active sites *via* strong adsorption, diminishing catalytic activity.[179] More adversely, gaseous products can cross over to the cathode, lowering the quality of H_2 and requiring additional purification processes. Those organic compounds are vulnerable to reacting with membrane materials, affecting the ionic conductivity and thereby causing degradation.[52]

As for natural seawater, it contains large amounts of dissolved gases such as nitrogen (N_2), oxygen (O_2), argon (Ar), *etc.* The concentration of those gaseous impurities ranges from nmol L^{-1} to μmol L^{-1}. Although chemically inert gases can hardly threaten the systematic performance, they will lower the H_2 quality to meet stringent standards.[52] Moreover, the variety of biological substances in seawater is often overlooked. Biofouling has been evidenced to clog the active sites and the pores of the membrane, triggering significant performance degradation.[180–182] To date, little research has been carried out to reveal the specific impact of biofouling on device components, as well as anti-biofouling measures. In addition, endogenous impurities are usually regarded as the species generated during the degradation process within the electrolyzer system. Although seawater typically undergoes simple

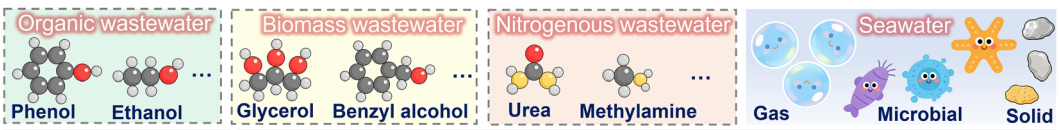

Non-ionic impurities	Main impact and potential challenges
Organics	Cell voltage: Replace OER with lower energy electrolysis
	Catalyst: Poison active sites with undesired adsorption
	Membrane: Degradation; affect the ionic conductivity
	Gas quality: Gaseous products cross over
Dissolved gases	Gas quality: Lower H_2 purity
Microorganisms	Catalyst & membrane: Biofouling induced degradation
Solid	Channel: Clogging issues with poor mass transfer

Fig. 5 Summary of the representative non-ionic impurities and impurity-induced challenges. Organic impurities, dissolved gas, microorganisms, and solids were introduced to analyze the frequently overlooked impact and potential challenges.

filtration to remove inert solid impurities (*e.g.*, sand and microplastic particles) before use, errors in system design and improper maintenance may also introduce solid impurities during long-term operation.[101] Concomitantly, those solid impurities in the electrolyte can continuously accumulate, thus obstructing porous transport channels and causing mass transfer issues.[52]

Therefore, it has been shown that both ionic and non-ionic impurities in distinct-grade water would pose enormous challenges to device components.[183] Simultaneously, it is urgent to develop an effective approach that not only minimizes the adverse impacts but also capitalizes on inherent impurities, realizing a win–win synergy of pollutant degradation and clean energy production.

2.2.4. Interfacial dynamic evolution. Real-world operating conditions, including seasonal, geographical, and environmental fluctuations, can potentially lead to significant dynamic evolution of impurities around the reaction microenvironment. Specifically, DIWE, driven by renewable energy, suffers from fluctuating power input.[184–186] Our group recently discovered that the cathode typically underwent oxidation when the reducing potential was discontinued. Due to pseudocapacitive properties of redox-active electrodes, halide ions (*e.g.*, Cl^- and Br^-) tended to adsorb onto the cathode during shutdown and discharge processes, causing catalyst deactivation.[112] More adversely, continuous consumption of fresh impure water during the DIWE process provokes a significant increase in salinity levels in the electrolyte, resulting in undesired interfacial corrosion.[187]

Stabilizing interfacial pH fluctuation occurring near the electrodes is another formidable challenge during the DIWE process. Due to the lack of abundant buffering agents and slow transfer of H^+ and OH^-, the ionic impurities alone in natural seawater (pH = 8.0–8.3) can hardly regulate the local pH gradient.[68] Rapid consumption of protons under high current density drives the local pH to increase remarkably, thus instigating the cationic impurities (*e.g.*, Mg^{2+} and Ca^{2+}) to form hydroxide precipitates. This knock-on effect, driven by interfacial dynamic pH variations, alters the concentration of ionic impurities and blocks the active sites, exacerbating performance degradation. Consequently, incorporating buffering agents and circulating electrolytes constitutes a key factor in modulating pH gradients.[188]

3. Scenario-oriented electrocatalyst development

Electrocatalysts are one of the most widely studied components.[189] To resist the influence of various impurities in complex environments, it is essential to develop cost-effective electrocatalysts based on diverse criteria.[190–192] In this section, by fully drawing on the theoretical framework of mature HPWE technology, the impurity-induced interplay on electrocatalyst design was reassessed for the DIWE process. Moreover, recently reported strategies targeting typical challenging scenarios are comprehensively reviewed, guiding the electrocatalyst development under complicated real-world conditions.

3.1. Undesired precipitation at the cathode

As the cornerstone in producing H_2, the HER consumes the dissociated H^+, thereby engendering an increase in local pH.[193] Platinum (Pt)-based materials are generally used as the cathode for commercial implementation owing to their optimal adsorption of hydrogen and outstanding stability.[194] Despite numerous efforts devoted to developing non-noble metal materials (*e.g.*, Ni, Co, and Fe) to replace the expensive Pt-based materials, there is still a large room for further improvement towards industrial deployment.[195] Regrettably, the development of cathodic catalysts toward DIWE is more challenging. Due to interfacial pH gradients, cationic impurities (*e.g.*, Mg^{2+} and Ca^{2+}) can react with residual OH^- to form unfavorable hydroxide precipitates at the cathode. Although the pre-treatment could remove those alkaline earth metals by simply introducing alkali additives to form hydroxide precipitates, this electrolyte refining process requires the additional cost of alkali (*e.g.*, US$ 800 ton^{-1} of potassium hydroxide, KOH).[69]

To overcome this knotty problem, promoting reaction kinetics and limiting local pH increase are key to obviating catalyst deactivation. To date, several strategies have been suggested to confine Mg^{2+} and Ca^{2+} or OH^- around the reaction microenvironment, empowering cathode anti-precipitation properties.[196] As shown in Fig. 6, Tang's group constructed a microscopic bubble precipitate traffic system (MBPTS) on the cathode to repel nearby inorganic precipitates by forming strong localized airflows.[109] An industrially-relevant stability at 500 mA cm^{-2} for 150 h was achieved to produce cheaper H_2. Qiao's group conceived a localized acidic microenvironment by

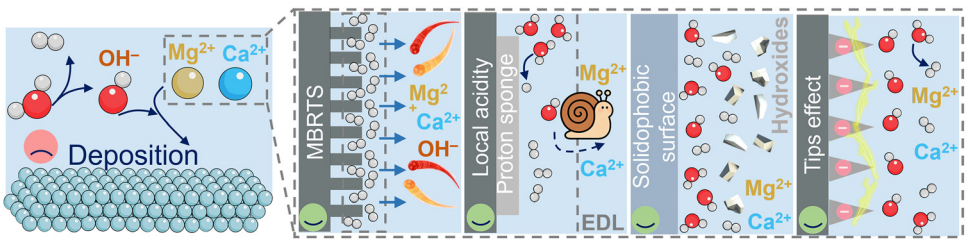

Fig. 6 Schematic illustration of strategies to inhibit undesired metal hydroxide precipitation on the cathode surface. Four commonly reported strategies, including the microscopic bubble precipitate traffic system (MBPTS), local-pH regulation, solidophobic surface, and tip effect, were summarized to reveal the metal precipitation at the cathode.

incorporating a tungsten oxide (WO_2) substrate, where a dynamic proton-buffering system was constructed.[197] The accumulation of OH^- was thereby inhibited with optimized adsorption energetics. This self-regulated proton regulation strategy enabled long-term operation at 100 mA cm^{-2} for 500 h. Regulating wetting properties and micro-nano morphologies was also shown as effective approaches for mitigating cathodic precipitation. Lu's group constructed a nanoconfined hydration layer between the electrode and precipitates, initiating hydration-mediated repulsive forces to suppress heterogeneous nucleation and scale adhesion.[198] Such a solidophobic strategy allowed stable operation over 1000 h in concentrated Ca^{2+}/Mg^{2+} solutions without conspicuous scale adhesion. Feng's group articulated a tip-effect-enhanced electrostatic repulsion strategy by creating nanostructures with high curvature on the cathode.[199] The enhanced electric field, evoked by the tip effect, suppressed the accumulation of OH^- on the electrode surface, thus alleviating metal hydroxide formation and preventing electrode clogging.

Notably, high-purity magnesium hydroxide ($Mg(OH)_2$) has a significant economic value (US$ 1000–1500 ton^{-1}) due to its widespread industrial applications.[200] The solidophobic strategy proposed by Lu's group has been regarded as an effective way to recover high-purity $Mg(OH)_2$ along with H_2 production.[111] Nonetheless, sufficient direct evidence from *operando* experimental observation is lacking to reveal how the Pt-I catalysts precisely control the local pH value within the range of Mg^{2+} precipitation (~9.3) and Ca^{2+} precipitation (~12.0). Therefore, metal resource recovery will help lower H_2 production costs, facilitating wider industrial deployment of DIWE technology.

3.2. Side reaction of chloride oxidation at the anode

The development of OER catalysts is also confronted with impurity-induced challenges. As mentioned in Section 2, the pH of the electrolyte is an essential factor in determining the selectivity of OER. In acidic conditions, the expensive iridium and ruthenium (Ir/Ru)-based catalysts are commonly used due to their stronger durability.[201] However, catalysts with OER activity (1.23 V *versus* the standard hydrogen electrode (SHE) at pH 0) are susceptible to the ClOR side reaction (1.36 V *versus* SHE at pH 0) at high applied potentials. In neutral media, the ClOR shifts to the HClO pathway with a broader potential window for the OER as compared to acidic conditions. Nonetheless, the OER process causes a local pH drop at the anode, making the ClOR more competitive. Highly alkaline conditions are more favorable for OER (0.40 V *versus* SHE at pH 14) as compared to the ClOR (0.89 V *versus* SHE at pH 14) in the DIWE process.[202–204] Unfortunately, corrosive ClO^- would form on the anode under high potential conditions, leading to unfavorable competition with the OER. This conspicuous impact may be attributed to active sites being shared by both ClOR and OER. Correspondingly, a two-electron transfer process with by-products can elicit catalyst poisoning or corrosion of the electrode. Beyond the requirement of high activity and stability, the Faradaic efficiency and selectivity of the anodic catalysts toward ClOR should be fully taken into consideration for the DIWE process.

To date, several strategies have been reported to alleviate the ClOR. As shown in Fig. 7, intensive studies have focused on incorporating the negatively charged layer (*e.g.*, PO_4^{3-}, SO_4^{2-}, MoO_4^{2-}, *etc.*) anchored onto the anode surface.[205–209] Leveraging electrostatic exclusion to repel Cl^- adsorption is conceived as the core function of those negatively charged layers. Moreover, Lewis acid oxides (*e.g.*, MnO_2, Cr_2O_3, V_2O_3, *etc.*) have been proposed to shield active sites from Cl^- attack and sustain OH^- enrichment.[210–212] This simple modification strategy has been regarded as an effective way to construct a local alkaline environment, which is conducive to enhancing both OER kinetics and resistance to Cl^- corrosion.[213] More ingeniously, Lu's group heralded a novel approach to capture free Cl^- *via* AgCl precipitation and subsequently suppress Cl^- adsorption. This common-ion repulsion effect significantly improved corrosion resistance, with negligible performance degradation over 5000 h at 400 mA cm^{-2}.[214] In addition, encapsulation of the metal active sites in armored shells, such as graphite, carbon nanotubes (CNT), manganese oxide (MnO_x), silicon oxide (SiO_x), and phthalocyanine, has recently garnered attention for preparing robust catalysts towards harsh real-world conditions.[215–221] When integrated with the above-mentioned methods, multifunctional protective layers could be constructed. Tang's group proposed a triple-protected design philosophy.[222] Filtering out Cl^- *via* PO_4^{3-} barriers and nano-sized MnO_2 alleviated corrosion issues. Tip-connected nanowires with cage-like architectures further minimized the physical destruction from the bubble impingement. Despite

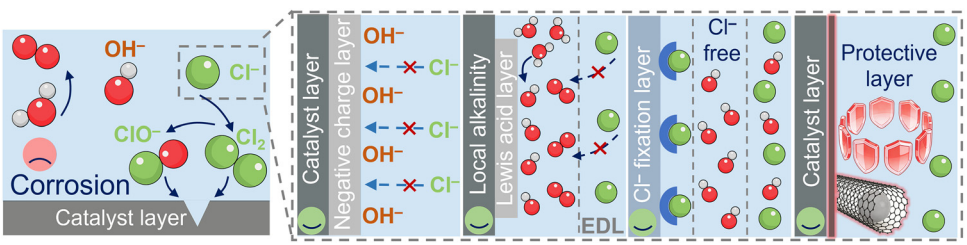

Fig. 7 Schematic illustration of strategies to repel Cl^- adsorption on the anode surface. Four commonly reported strategies, including negative charge layer modification, local-pH regulation, Cl^- fixation, and protective layer construction, were summarized to reveal the side reaction of chloride oxidation at the anode.

various methods developed to mitigating Cl^- corrosion, dense metal oxide layers might obstruct active sites with limited OER activity. More adversely, anions might suffer from depletion under high current density owing to gas evolution and electrolyte flow. Therefore, it is essential to design electrocatalysts that can maintain high activity, durability, and selectivity for industrial-scale deployment.[223]

3.3. High-potential dissolution at the anode

Improving the working potential of OER catalysts is crucial for enhancing water splitting efficiency and cutting costs. Unfortunately, the high-potential dissolution issues (thermodynamic material instability) of OER catalysts can hardly be overlooked under intricate reaction microenvironments.[224] Unlike HPWE, DIWE is affected by the dual challenges of impurity corrosion and high-potential dissolution. Specifically, due to the *in situ*-formed highly active Ni/Co hydr(oxy)oxide phases with tunable electronic structure achieved by Fe^{3+} incorporation, Ni/Co-Fe layered double hydroxides (LDHs) have been regarded as the benchmark of non-noble metal catalysts in alkaline media.[225–228] However, these highly active OER catalysts suffer from dissolution under high potential conditions. As shown in Fig. 8a, Markovic's group discovered a dynamically stable interface with dissolution and redeposition of active sites.[229] In Fe-free electrolytes, an 80% decline in OER activity was observed alongside a roughly 80% loss of iron species from the catalyst surface. Intriguingly, when tests were performed in an electrolyte with 0.1 ppm Fe, no conspicuous changes in the catalysts were found. Concomitantly, even a modest activity enhancement was detected. The subsequent experiments on the ternary hydr(oxy)oxides (M_1–M_2–M_3–O_xH_y) further elucidated that OER activity monotonically increased according to the 3d transition metal family, following the order: Ni–Fe–Cu > Ni–Fe > Ni–Fe–Co > Ni–Fe–Mn. This improved OER activity was ascribed to the enhanced Fe adsorption, thus entailing a higher surface concentration of Fe active sites.

Beyond leveraging metal cationic impurities to strengthen dissolution resistance, Sun's group pioneered single-anion engineering to tailor the interlayer and surface of the LDH-based materials.[110] The layered and positively charged nature of LDH-based materials facilitated anion intercalation. Initiated by a low applied electric field, hexafluorophosphate (PF_6^-) could easily intercalate into the interlayers and adsorb onto the surface of the Ni–Fe LDHs, as shown in Fig. 8b. PF_6^- exhibits weak coordination with Fe sites, inhibiting undesired Fe segregation. The accumulation of PF_6^- ions further excludes Cl^- penetration during the seawater oxidation process. This bifunctional design philosophy maintained stable operation over 5000 h.

Notably, electrolyte-induced strategies, such as utilizing Cl^-, have recently been reported to stabilize the active sites.[230] Despite being traditionally regarded as harmful anionic impurities in the DIWE system, the positive role of Cl^- was uncovered by Qiao's group.[231] According to the *operando* spectroscopic results, the specific adsorption of Cl^- on Fe sites

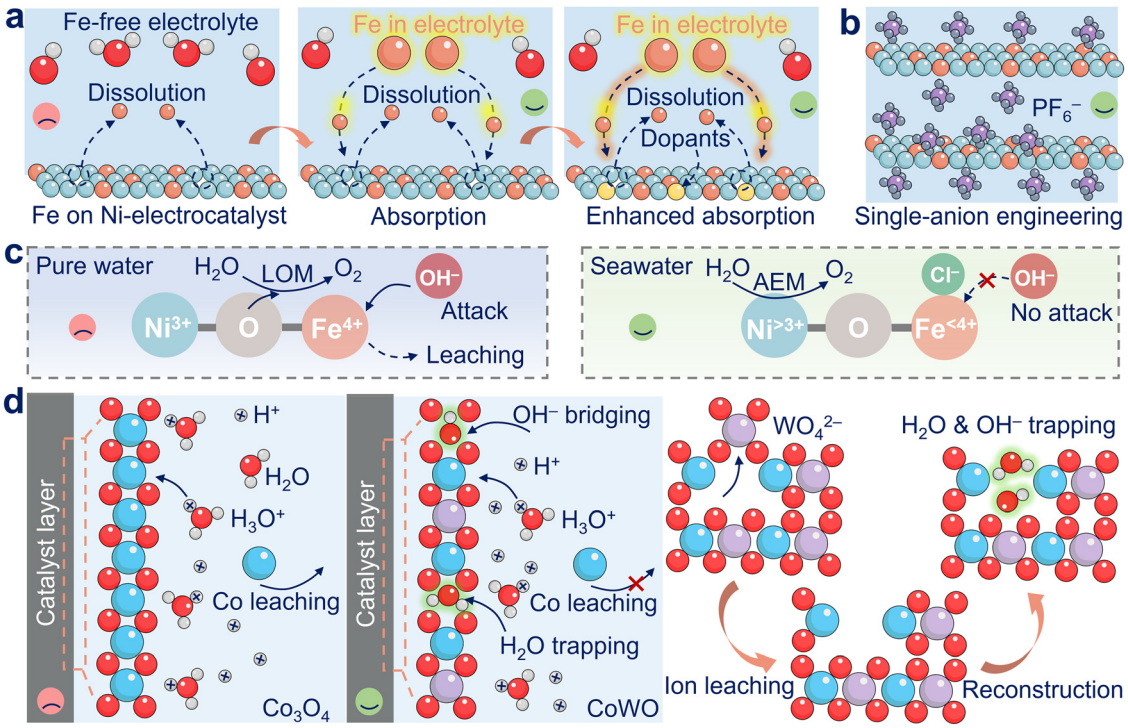

Fig. 8 Schematic illustration of the effect of ionic impurities in the electrolyte on the degradation of hydr(oxy)oxide OER catalysts. (a) Fe impurity-induced dissolution and readsorption. Adapted with permission from ref. 229, copyright 2020 Springer Nature. (b) Interlayer and surface adsorption of PF_6^-. Adapted with permission from ref. 110, copyright 2025 Springer Nature. (c). Utilization of Cl^- to stabilize the active sites. Adapted with permission from ref. 231, copyright 2023 John Wiley & Sons, Inc. (d) Water-hydroxide trapping strategy to suppress Co dissolution. Adapted with permission from ref. 86, copyright 2024 American Association for the Advancement of Science.

could enhance the valence of Ni and lower Fe valence. As shown in Fig. 8c, driven at high potential, the increased Fe valence becomes a hard acid and is easily attacked by OH^- (hard base), resulting in unwanted leaching and poor durability. In alkaline seawater, however, the leaching could be suppressed by the protection of adsorbed Cl^-. Meanwhile, increased Ni valence and the transition from the lattice oxygen mechanism (LOM) to the adsorbate evolution mechanism (AEM) were further verified to be responsible for the enhanced OER activity. Analogously, the cobalt-based oxides (CoO_x) are regarded as a promising alternative to expensive Ir/Ru catalysts for acidic OER. Nonetheless, as shown in Fig. 8d, Co_3O_4 is prone to H^+/H_3O^+ attack with severe Co ion dissolution in acidic media. In this regard, Arquer's group successfully incorporated the high-valence sacrificial element tungsten (W) to form a $CoWO_4$ (CWO) crystal structure.[86] This sacrificial element could be selectively removed by the water-hydroxide-WO_4^{2-} anion exchange process, subsequently evoking structural delamination, trapping, and stabilization of water-hydroxide in the defect network. This water-hydroxide shielding strategy inhibited Co ion dissolution and achieved stable operation for 608 h at 1000 mA cm^{-2}.

3.4. Anodic oxidation of organic impurities

Owing to sluggish four-electron-transfer kinetics with a high theoretical potential (1.23 V *vs.* the reversible hydrogen electrode (V_{RHE})), it is impractical for OER catalysts to completely circumvent detrimental competition with the ClOR.[232] To fix this bottleneck issue, the hybrid electrolysis strategy paves the way for breaking the limit of OER. Since rich organic impurities already exist in some wastewater sources, it is highly possible that these organic molecules can be oxidized at a lower potential to replace OER at the anode.[233] Qiao's group developed a Co-doped Cu_3P catalyst as both the anode and cathode to couple seawater electrolysis with formaldehyde (HCHO) oxidation. As shown in Fig. 9, the theoretical potential of partial oxidation to generate formate is only −0.22 V_{RHE}, remarkably negative compared to the OER (1.23 V_{RHE}).[234] More subtly, integrating seawater electrolysis with upcycling of polyethylene terephthalate (PET) waste was reported by Chen's group.[235] The as-prepared Pd–$CuCo_2O_4$ catalyst boosted the adsorption of PET-derived ethylene glycol (EG) and subsequently facilitated the partial oxidation to form GA. This EG-to-GA process manifested an ultralow theoretical oxidation potential (0.065 V_{RHE}), effectively obviating corrosion of the anode. Analogously, abundant urea-bearing wastewater acts as another promising candidate for oxidation at the anode for energy-saving.[236] Urea is detected as the main component of urine (~150–580 mM) with favorable theoretical oxidation potential (0.37 V_{RHE}).[237] Aside from this organic impurity in urine, large amounts of ionic impurities, such as Cl^- (~40–280 mM), SO_4^{2-}, NH_4^+, PO_4^{3-}, and Ca^{2+} (~2–56 mM), were present.[238] Notably, the rich Cl^- impurities in urine can also give rise to the degradation of the electrode. In this regard, Qiao's group claimed an interfacial microenvironment strategy by leveraging a Lewis acid to modify Ni phosphide catalysts.[239] The as-prepared catalysts required only 1.62 V to reach the current density of 3000 mA cm^{-2} and exhibited a long-term durability for 1000 h. As compared to the electrooxidation of urea with carbon emissions, hydrazine oxidation (HzOR) possesses a negative theoretical oxidation potential (−0.33 V_{RHE}). Besides, the electrooxidation of hydrazine-rich industrial wastewater can further alleviate environmental

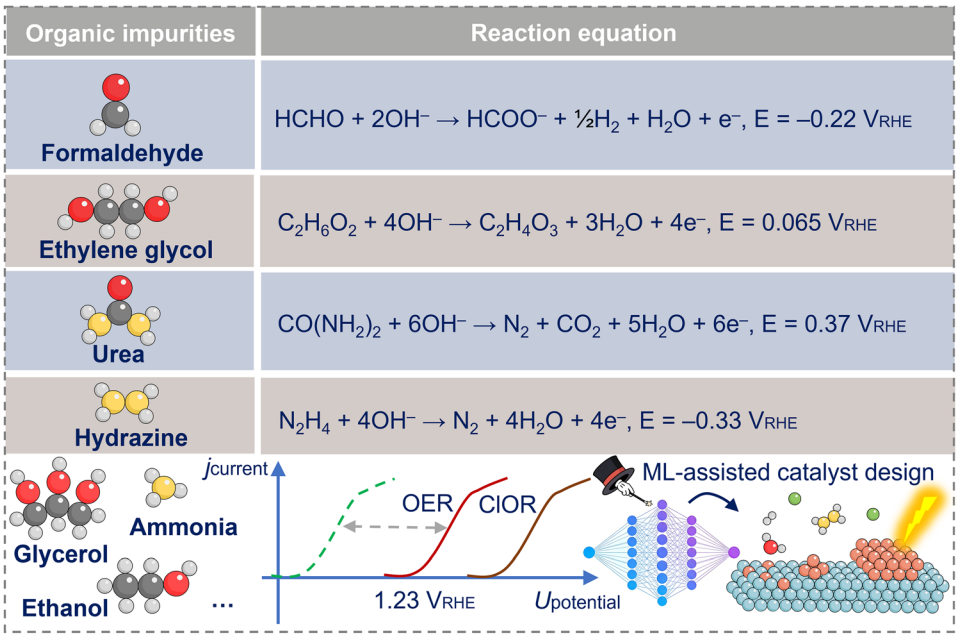

Fig. 9 Summary of the representative organic impurities and their theoretical oxidation potential. Commonly reported organic impurities, including but not limited to formaldehyde, ethylene glycol, urea, hydrazine, *etc.*, were summarized with the lower theoretical potential to replace the OER. Additionally, ML-assisted catalyst design was suggested to accelerate the development of organic oxidation reactions.

pollution. Qiu's group integrated HzOR with neutral seawater electrolysis.[240] The as-prepared NiCo/MXene-based catalyst showcased a low electricity expense of 2.75 kWh m^{-3} H_2 at 500 mA cm^{-2}, reducing the energy input by 48% in contrast to commercial alkaline water electrolysis.

Although substantial progress has been made by utilizing diverse organic impurities to assist H_2 production, a severe challenge is to separate and purify the products from the electrolyte. Due to a wide range of organic impurities in distinct-grade wastewater, the impurity-induced interference merits sufficient attention. Furthermore, it is laborious to develop the optimal catalyst for hybrid electrolysis based on trial-and-error practice. This labor-intensive field usually involves time-consuming experimental synthesis and evaluation, deeply relying on the chemical intuition of investigators. In this context, applying machine learning (ML) could be an effective tool to manage complex systems with multiple variables.[241] This new research paradigm aims to figure out hidden correlations among high-dimensional datasets, filling the gap between simplified models and optimal catalysts for multiple electrooxidation reactions of organics. However, ML-driven electrocatalyst design has barely been touched upon in this field. High-fidelity datasets and reliable ML models are required to help researchers wisely choose synthesis recipes of the catalysts according to the specific scenario.

4. Function-oriented electrolyzer development

Despite substantial efforts devoted to catalyst development, further innovation of the functional electrolyzer is indispensable for the abovementioned challenging scenarios.[160] As compared to the HPWE technology, electrolyzer design for DIWE is confronted with a pyramid of interconnected issues provoked by various impurities. In this section, building upon the recently reported advances in this field, mature membrane-based water electrolyzers were first elucidated. The notable knowledge gap between the specific impact of impurities and the membrane degradation mechanism was bridged. The emerging novel design philosophy was subsequently reviewed to develop functional electrolyzers for the DIWE system.

4.1. Membrane-based electrolyzer

Membrane-based electrolyzers are commonly leveraged to separate the gaseous products from the cathode and anode (H_2 and O_2), involving proton exchange membrane water electrolyzers (PEMWE), alkaline water electrolyzers (AWE), anion exchange membrane water electrolyzers (AEMWE), and bipolar membrane water electrolyzers (BPMWE). The crossover of active species can be obviated, concomitantly achieving higher current density by minimizing ohmic losses.[96] Notably, there is growing interest in improving membrane technology to meet the requirements of the DIWE process.[100] However, engendered by uncontrolled migration of impurities, membranes are fragile and even deteriorate before other electrolyzer components. In this context, a more efficient and feasible functional membrane-based electrolyzer is instrumental in scaling up DIWE.[97]

4.1.1. PEMWE. Emerging from NASA's space programs in the 1960s, PEMWE is expected to account for 40% of the green H_2 market.[242] In the commercial PEMWE-based system, the expensive cathode (*e.g.*, Pt) and anode (*e.g.*, iridium oxide(IrO_2)) are separated by a costly Nafion membrane that is composed of PFSA polymers.[119] As shown in Fig. 10, the H^+ goes through the membrane and couples with electrons at the cathode to form H_2. This simple configuration enables high current densities (up to 3000 mA cm^{-2}) and exhibits fast dynamic response, highlighting its strong potential for industrial-scale production of high-purity H_2 (>99.9%).[243–245] Regrettably, stringent requirements for water purity impose enormous challenges for the application with impure feedwater. Although the insoluble hydroxides could be effectively suppressed at the cathode under acidic conditions, the Nafion membrane is extremely sensitive to cationic impurities (*e.g.*, Na^+ and Fe^{2+}). The proton conductivity would be severely jeopardized by those cationic impurities during long-term operation. Additionally, most metal catalysts suffer from dissolution in acid medium with poor durability.[246] Restricted choices among noble metal catalysts further elevate capital expenditure in PEMWE systems.[247] More adversely, the competing ClOR in acid conditions deteriorates OER selectivity, provoking unwanted corrosion in device components. Collectively, the above negative factors contribute to the poor lifespan of PEMWE toward industrial-scale DIWE application.

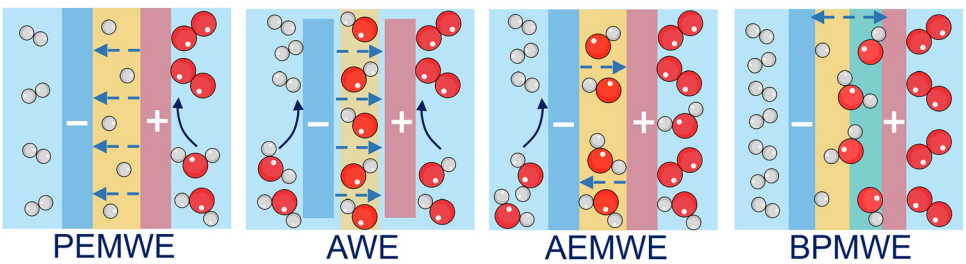

Fig. 10 Schematic illustration of the configuration of membrane-based electrolyzers. Four commonly reported membrane-based electrolyzer configurations, including PEMWE, AWE, AEMWE, and BPMWE, were summarized to reveal the challenges toward the DIWE process. The characteristics of each membrane-based electrolyzer were introduced in terms of cell configuration and ion transport.

4.1.2. AWE. Commercialized since the 1950s, AWE has become one of the most widely employed electrolyzers for large-scale hydrogen production.[116] Electrodes, comprising non-noble metal-based materials (*e.g.*, Ni, Co, Fe), are separated by the porous diaphragm (*e.g.*, Zirfon).[248] Liquid alkaline electrolyte (*e.g.*, 30–40% KOH) is thereafter incorporated into the two-compartment cell. Generally, H_2O is split into H_2 and OH^- at the cathode. OH^- subsequently passes through the porous diaphragm and is ultimately oxidized at the anode to form O_2. As compared to the PEMWE, AWE is well-suited to be scaled up owing to the utilization of low-cost catalysts and non-ion-exchange membranes.[249] Also, the alkaline environment creates the conditions for pre-treatment to remove Ca^{2+}/Mg^{2+}. The OER selectivity could also be enhanced in alkaline media. Those advantages of the AWE hold great potential to be applied in the DIWE system. Nonetheless, the inherent cell configuration impedes the operation at large current densities. High permeability can lead to uncontrolled ion migration, such as Na^+, H^+, OH^-, and Cl^-. The wide range of impurities further imposes challenges related to membrane blockage and gas crossover.[250]

4.1.3. AEMWE. Combining the advantages of PEMWE and AWE, AEMWE has attracted more attraction for application in the DIWE system.[251] Water is reduced at the cathode with the formation of H_2 and OH^-. The OH^- thereafter migrates through the AEM and is oxidized to O_2 at the anode. When moving to a larger-scale system for industrial implementation, water is usually supplied to the anode to collect high-purity H_2 at the cathode. The AEM, with the inherent water uptake and transport properties, allows water to pass from the anode to the cathode. The OH^- generated from the splitting of H_2O can subsequently return to the anode.[90] Operating in alkaline environments with high ion conductivity, AEMWE can use non-noble-metal catalysts to achieve large current densities without conspicuous gaseous crossover. The activity and selectivity of OER would further be enhanced in the alkaline medium. Unfortunately, inevitable Cl^- crossover through the AEM would facilitate the formation of ClO^- and anode corrosion.[252] When directly supplying chloride-rich feedwater to the anode, unwanted ClOR and corrosion risks would be intensified.

4.1.4. BPMWE. Building upon the above discussion, the dynamic evolution of the local pH environment imposes persistent challenges. In this context, BPMWE, comprising AEM and PEM, has been designed to achieve the optimal pH environments for each half-reaction.[253,254] Water is split at the interface between AEM and PEM.[255] The undesired ClOR would be suppressed at the anode by the local alkaline environment with the use of AEM. Concurrently, the precipitation of hydroxides can be suppressed at the cathode by the local acidic environment generated by the proton flux from the PEM. Integrating the merits of PEMWE and AEMWE, BPMWE is regarded as a promising candidate for the DIWE system. Regrettably, impurity-induced impact can potentially impede its further scalability. BPM is susceptible to inorganic and organic impurities. The degraded ion conductivity would result in poor durability over long-term operation. Similar to AEMWE, when a chloride-rich electrolyte is directly supplied to the anode, corrosion risks and the ClOR at high potentials remain unresolved. Correspondingly, degradation mechanisms and strategies necessitate further investigation to adapt the BPMWE to the DIWE system.

4.2. Novel functional electrolyzer

Based on the discussion of conventional membrane-based electrolyzers, it is concluded that they share common issues elicited by impurities. The overwhelming focus on catalysts often overshadows the equally critical role of other device components. On this point, an efficient and sustainable DIWE system is supposed to possess facile device configurations with suitable components. Different grades of feedwater can be supplied as an electrolyte with minimal treatment. An industrial-scale current density with low energy consumption is expected to be sustained without conspicuous degradation over long-term operation. Consequently, to develop novel functional electrolyzers toward the DIWE process, a series of design strategies is comprehensively reviewed in this section.

4.2.1. Direct and indirect water-vapor electrolysis cells. As shown in Fig. 11a, distinct from conventional water-liquid electrolysis (WLE), solid oxide electrolysis cells (SOEC), operating at high temperature (400–800 °C), directly split water vapor at the cathode to form H_2 and O^{2-}.[256–258] The O^{2-} subsequently passes through the solid oxide electrolyte to the anode and is ultimately oxidized to O_2. In contrast to the abovementioned membrane-based electrolyzers, gaseous water molecules are supplied into cells instead of aqueous feedwater.[259] This inherent merit of water-vapor electrolysis (WVE) potentially separates water from other impurities (*e.g.*, Cl^-, Ca^{2+}, Mg^{2+}). Also, the introduced thermal energy input allows a higher electrolysis efficiency. Despite its notable merits over conventional electricity-driven electrolyzers that operate below 100 °C, the higher operating cost associated with high-temperature working conditions imposes limitations on its widespread application. High operating temperature engenders a limited range of catalysts with high thermal stability. Furthermore, even a trace amount of salt particle contaminants, mixed with the gas flow, can potentially clog the inlet and result in system failure.[90] Accordingly, these device-level challenges necessitate a suitable gas flow design and pre-treatment strategies to preclude potential performance degradation.

To circumvent the limitations brought by high temperature, as shown in Fig. 11b, low-temperature (<100 °C) WVE has garnered extensive attention. Logan's group proposed the vapor-fed anode configuration coupled with a saltwater catholyte.[260] The humidified gas stream is directly pumped into the anode with the generation of protons and oxygen. The formed protons subsequently migrate through the PEM to the cathode chamber. The water required at the anode is supplied by the water vapor, as well as the water diffusing from the saltwater catholyte through the membrane. This unique configuration for saltwater electrolysis exhibited comparable performance to a conventional PEMWE. More beneficially, the

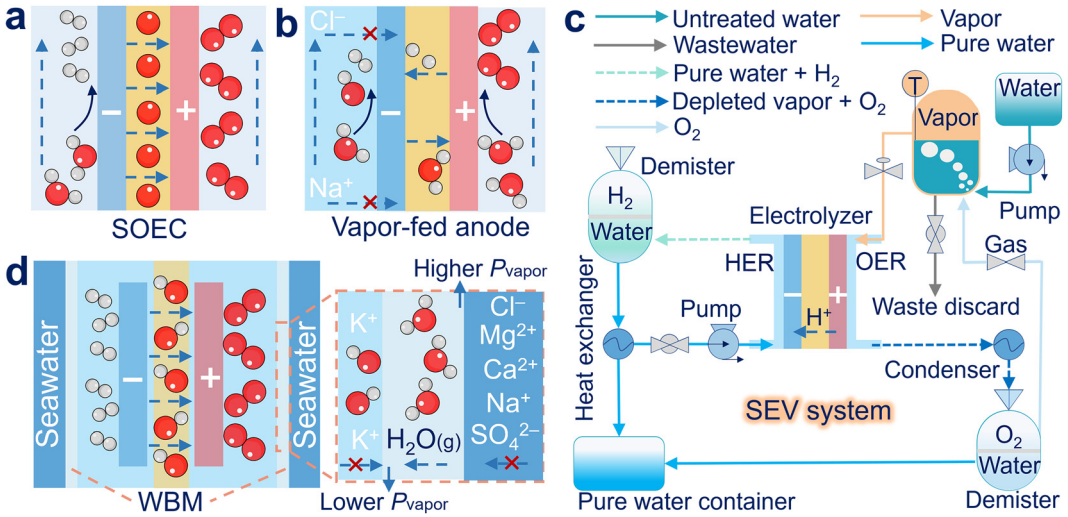

Fig. 11 Schematic illustration of the direct and indirect water-vapor electrolysis cell. (a) SOEC. (b) Vapor-fed anode. Adapted with permission from ref. 260, copyright 2025 Royal Society of Chemistry. (c) Process flow chart of the SVE system. Adapted with permission from ref. 261, copyright 2024 Royal Society of Chemistry. (d) WBM. Adapted with permission from ref. 262, copyright 2022 Springer Nature.

migration of Cl^- from cathode to anode is prevented by the charge repulsion of the PEM. Pronton transfers from the anode and alleviates the undesired migration of Na^+ through the PEM. As shown in Fig. 11c, Shao's group further introduced a semi-vapor electrolysis (SVE) system based on the PEMWE technology.[261] In this SVE system, low-temperature vapor electrolysis takes place at the anode while liquid water is circulated at the cathode. Notably, the generation of ultrapure water vapor from non-volatile impurities (*e.g.*, salts, precipitation, *etc.*) creates the possibility of direct electrolysis of various impure water sources. By recycling O_2 products as the vapor carrier gas, performance identical to that obtained using N_2 or air was measured. More favorably, the sufficient waste heat generated during the electrolysis process could be a suitable energy source for low-temperature vapor production, while simultaneously yielding pure water as a by-product. The above optimized workflow further mitigates energy consumption and system complexity.

Intriguingly, as shown in Fig. 11d, Xie's group introduced a hydrophobic porous waterproof breathable membrane (WBM) to separate the seawater and self-damping electrolyte (SDE).[262] The interfacial vapour pressure (P_{vapor}) difference enables the escape of water vapor from seawater to SDE, without extra energy consumption. The water vapor is subsequently re-liquified by the adsorption of the SDE. As an indirect WVE process, water vapor is converted into pure water for subsequent electrolysis. In contrast to the above direct WVE system, this novel electrolysis configuration relies on a self-driven phase transition mechanism, realizing *in situ* water purification and electrolysis processes. The impurity-induced challenges during the DSE process are effectively ameliorated. Nonetheless, the optimal working temperature (70–90 °C) for vapor-phase water transfer impedes the direct utilization of natural seawater in offshore regions. Concurrently, the deployment of a strongly alkaline electrolyte potentially poses a threat to the ocean ecosystem due to the occurrence of uncontrolled leakage under unexpected fluctuations.

4.2.2. Novel ionic-conducting electrolyzer. Alternatively, developing novel ionic-conducting electrolyzers has become an effective tool to sustain ionic balance and inhibit the unfavorable crossover.[263–266] As shown in Fig. 12a, Qiao's group proposed an ion-selective gate (ISG) strategy toward the electrolysis of impure water.[267] This facile configuration features the direct coating of commercial catalysts with ionomers. At the cathode, anion-selective ionomers boost the OH^- migration and prevent cationic impurities (*e.g.*, Ca^{2+}/Mg^{2+}) from forming hydroxide precipitates. At the anode, cation-selective ionomers enhance the H^+ migration and prevent the Cl^- attack. The stable interface across both electrodes exhibits broad applicability for diverse impure water sources. However, this ISG-based electrolyzer still lacks degradation monitoring to deal with unexpected perturbations under intricate environments, necessitating further enhancement to sustain the durability and selectivity.

Designing novel ion exchange membranes also plays a crucial role in improving the electrolyzer performance. Cation exchange membranes (CEM) are known for selectively allowing cations, particularly Na^+, to go through during the DIWE process.[268] Recently, by utilizing the Na^+-conducting membrane, Li's group has developed an asymmetric electrolyzer with a dual electrolyte configuration.[269] As shown in Fig. 12b, sodium hydroxide (NaOH) is selected as the anolyte. Meanwhile, the natural seawater serves as the catholyte. Driven by the applied potential, OH^- is converted to O_2 at the anode. Na^+ subsequently passes through the Na^+-conducting membrane from the anode to the cathode. Concurrently, H_2 and OH^- are formed at the cathode. This novel asymmetric configuration suppresses Cl^- migration to the anode, preventing the undesired ClOR. More beneficially, the circulation of seawater alleviates the fluctuation of local pH, deterring the unwanted hydroxide precipitation at the cathode.

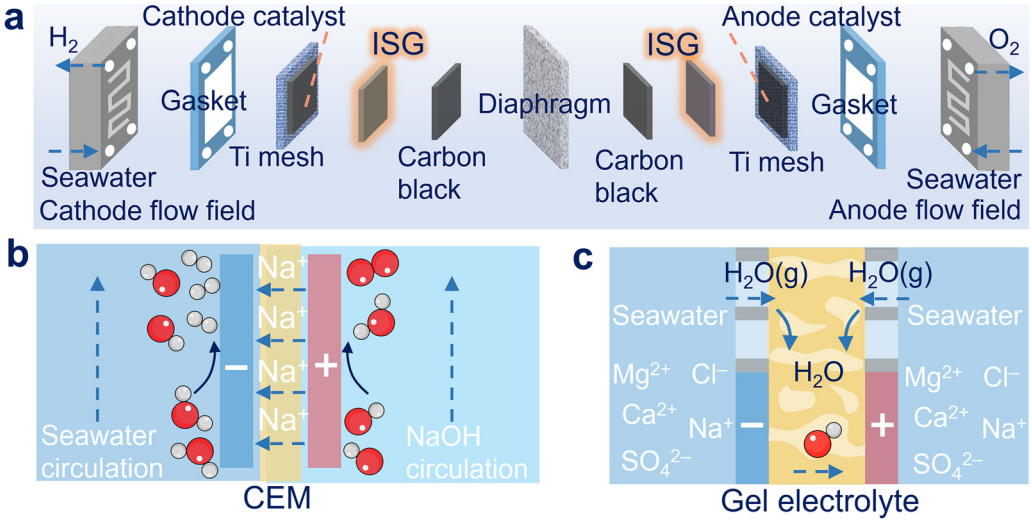

Fig. 12 Schematic illustration of novel ion-conducting configurations. (a) ISG. Adapted with permission from ref. 267, copyright 2025 Springer Nature. (b) CEM. Adapted with permission from ref. 269, copyright 2023 Springer Nature. (c) Gel electrolyte. Adapted with permission from ref. 271, copyright 2025 Royal Society of Chemistry.

However, intricate environments pose greater threats to the durability and selectivity of the CEM, inducing unexpected ionic crossover and electrolyte leakage. These risks might eventually cause failure of system performance. Therefore, periodic evaluation during electrolysis, including real-time monitoring of membrane fouling and electrolyte leakage, is crucial, particularly with the aid of ML model predictions.[270]

Concerning the strong alkaline electrolyte leakage, Xie's group further improved their previous strategy by incorporating the gel electrolyte.[271] As shown in Fig. 12c, the external seawater is isolated from the internal electrode and the gel electrolyte by deploying hydrophobic breathable membranes. In this optimized configuration, the gel electrolyte, made of KOH modified polyvinyl alcohol (KOH-PVA), is shown to conduct ions, mediate water migration, and prevent gas crossover. The vapor pressure difference between the gel electrolyte and seawater drives the migration of water vapor from the seawater to the gel electrolyte. Induced by concentration gradients, water molecules arrive at the electrode through dissociation and association with the OH^- ions in the gel. The water is ultimately split into O_2 at the anode and H_2 at the cathode. Concomitantly, the OH^- in the gel migrates from the cathode to the anode with the formation of an ion pathway. The as-prepared gel electrolyte manifested the capability of producing H_2 directly from the humidified gas atmosphere over 220 h. Regrettably, gel-based materials are inherently vulnerable to dehydration under high-temperature and dry environments, thereby triggering the alteration of their physicochemical properties.[272–274] Given the unexpected perturbation in real-world environments, there is still a large gap before extensive industrial applications.

4.2.3. Novel membraneless electrolyzer. Building upon the above discussion, employing membranes or similar functional media plays an essential role in inhibiting the hazardous mixing of H_2 and O_2. However, their degradation under complex conditions is also identified as the main source of system failure. Accordingly, the membraneless electrolyzer has emerged as a promising alternative to reduce capital investment costs and enhance the lifespan of the system.[275] To ameliorate the membrane dependence, the conventional methods mainly focus on the optimization of cell configurations with the specific flow-field designs and bubble management. For example, as shown in Fig. 13a, buoyancy forces are employed in an angled cell to drive O_2 and H_2 bubbles into gas reservoirs.[276] More intriguingly, as shown in Fig. 13b, fluid dynamic forces are deployed in microfluidic cells to trigger laminar flows of O_2-containing anolyte and H_2-containing catholyte that ultimately separate in the T-shaped channels.[277] As shown in Fig. 13c, flow-through cells are further designed to drive the flows of the anolyte and catholyte through porous anodes and cathodes to realize the separation of O_2 and H_2.[278]

Recently, decoupled water electrolysis (DWE) with the supply of the same electrolyte in undivided cells has garnered extensive attention for membraneless electrolysis.[279] In the DWE system, solid-state redox mediators are usually introduced as auxiliary electrodes, temporally and spatially regulating the exchange of H^+ or OH^- with the cathode and anode.[280] For instance, Yang's group developed a decoupled seawater direct electrolysis (DSDE) system with a membrane-free configuration and desalination-free operation.[281] They employed TQBQ-COF (Covalent Organic Framework) as a solid-state redox mediator to successfully decouple the HER and ClOR in acidic conditions. As shown in Fig. 13d, coupling with ClOR at the anode, the COF-based mediator first undergoes protonation. Subsequently, it deprotonates to couple with HER at the cathode. This spatial and temporal isolation of the production of H_2 and high-value Cl_2 circumvents the use of costly and fragile PEM, demonstrating promising compatibility with seawater. Regrettably, the solid-state redox mediators potentially suffer from limited capacity and rate, necessitating regeneration in the batch process.[282] In this regard, the soluble redox mediators have emerged. As shown in

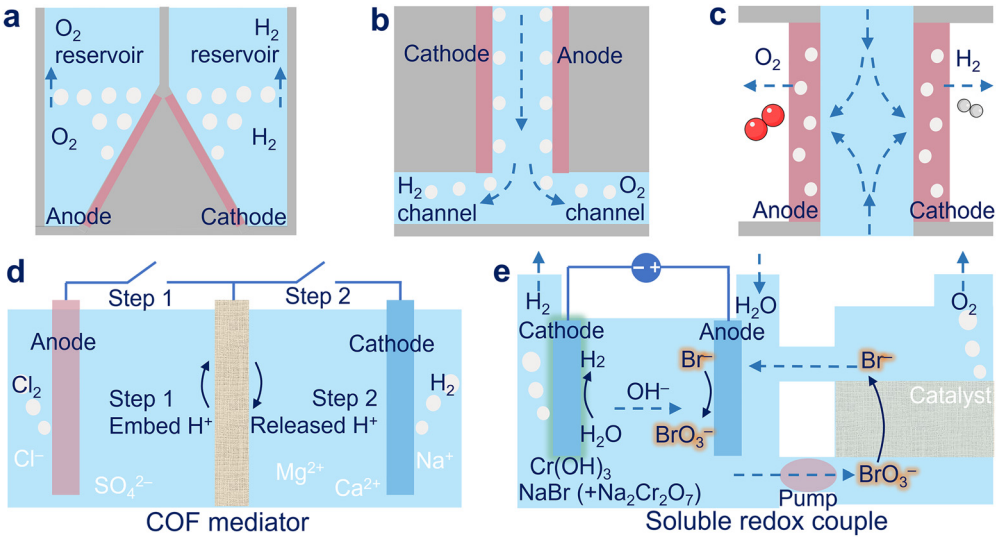

Fig. 13 Schematic illustration of the configuration of membraneless electrolyzers. (a) Angled electrolysis cells. Adapted with permission from ref. 276, copyright 2018 Elsevier. (b) Microfluidic cells based on the Segré-Silberberg effect. Adapted with permission from ref. 277, copyright 2015 Royal Society of Chemistry. (c) Divergent electrode-based flow through cells. Adapted with permission from ref. 278, copyright 2015 Elsevier. (d) COF mediator-based decoupled water electrolysis. Adapted with permission from ref. 281, copyright 2025 John Wiley & Sons, Inc. (e) The bromide/bromate decoupled water electrolysis. Adapted with permission from ref. 283, copyright 2024 Springer Nature.

Fig. 13e, Rothschild's group proposed a bromide/bromate (Br^-/BrO_3^-) redox couple to facilitate H_2 and O_2 production in separate electrolytic and catalytic cells.[283]

In this novel cell configuration, the BrO_3^- migrates from the electrolytic cell to the catalytic cell, where it is catalyzed to bromide and subsequently moves back to the electrolytic cell. More ingeniously, the cathode coated with a semipermeable thin layer of chromium hydroxide ($Cr(OH)_3$) could prevent the reduction of BrO_3^-, sustaining the HER activity. Despite the merits of the DWE system, the inherent characteristics of discrete water electrolysis, such as two subprocesses in separate cells or sequentially in different stages, increase the complexity of electrolyzer development. More adversely, only a few DWE systems with larger stacks can achieve ampere-level current density, impeding the cost-competitive prospects as compared to conventional electrolyzers.[282] The lower energy efficiency induced by excess voltage might be a warning for researchers to reconsider the suitable redox mediators for large-scale implementation.[284,285]

5. Pathway of DIWE: from lab to industry

To date, numerous studies have been reported on green H_2 production, with particular emphasis on DIWE technology. However, the majority of those works prioritize the development of highly active catalysts or the optimization of a single device component. Such a narrow focus on individual components has overshadowed the equally vital importance of coherent industrial-scale process integration. Therefore, bridging the gap between textbook knowledge and industrial deployment remains far from complete. In this section, we identify requirements for device components (*e.g.*, electrocatalysts, membranes, electrolyzers) at an industrial scale. Electrolysis system integration and synergistic optimization for realizing full-chain improvement are emphasized in real-world application scenarios.

5.1. Gap between lab findings and industrial application

In the laboratory, the traditional membraneless and H-type electrolyzers with limited catalytic areas (1 cm^{-2}) are usually employed for feasibility verification. The most frequently used metrics are the overpotentials at a certain current density (*e.g.*, 10 mA cm^{-2}) to evaluate the activity of the as-prepared catalysts. Ultrapure water (18.2 MΩ cm) is used to prepare simulated seawater by adding defined chemicals, such as sodium chloride (NaCl) solutions.[269] Optimal catalyst formulations are selected based on the criteria of minimal overpotential or maximal stable operating time. Unfortunately, lab findings can hardly be applied to direct industrial implementation. As shown in Fig. 14a, a broad range of impure water sources, including tap water, wastewater from municipal, industrial, and agricultural sources, natural seawater, *etc.*, interfere with device components. Practical hurdles, involving scaling, fouling, and upkeep, remarkably impede large-scale applications. For example, Xie's group presented a scaled floating platform under a fluctuating ocean environment.[113] This pilot system, based on their previously reported phase-transition strategy, showcased an electrolysis capacity of 6 kW, a hydrogen production rate of 1.2 $Nm^3\ h^{-1}$, an energy consumption of 5 kWh Nm^{-3} H_2, a high purity of H_2 (99.99%), and a stable operating time of 240 h in Xinghua Bay. However, contamination and wetting of the membrane were discovered during long-term operation. The attachment of microorganisms or scaling

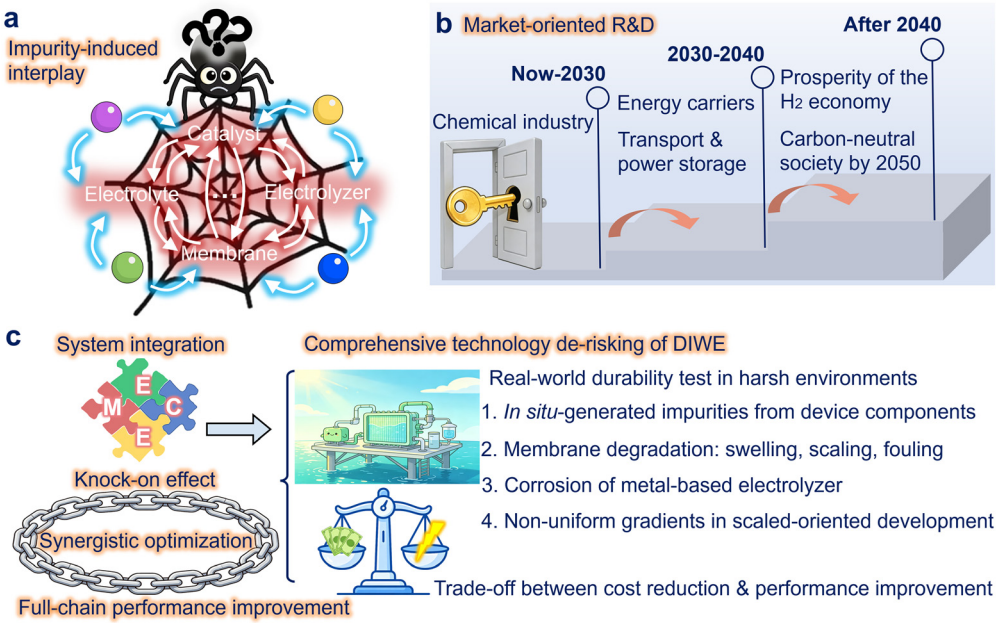

Fig. 14 Schematic illustration of the pathway from lab to industry. (a) Impurity-induced interplay on each device component. (b) Three stages of market demand: now to 2030, 2030–2040, and after 2040. (c) What is actually required for industrial applications: system integration and synergistic optimization for realizing performance improvement across the full chain in real-world application scenarios.

significantly degraded the water migration ability, aggravating membrane aging and increasing subsequent upkeep costs.[204]

Additionally, cationic species exhibit a stronger thermodynamic affinity to PFSA than protons, thus resulting in coordination with sulfonate groups ($-SO_3^-$, PFSA functional groups) and replacing protons through ion exchange, eventually diminishing proton conduction through the membrane.[286] More critically, as only protons are consumed for HER, cations would accumulate with a concentration gradient at the cathode. The applied electric potential must drive those cations against the concentration gradient, thus raising the membrane potential needed for ion transport. Collectively, these factors increase the cell resistance and jeopardize the stability of the electrolyzer. To mitigate the undesired impact of cationic impurities, Ren's group proposed the approach of acidifying reclaimed water (RW) to boost proton availability for RW electrolysis. The excess protons were evidenced to facilitate the proton migration and suppress cation interference. Stable operation was demonstrated for 300 h at 150 mA cm^{-2}. This acidification step eliminated multi-stage RW pre-treatment, cutting costs by 46.9% and energy intensity by 61.8%. Analogously, Ling's group proposed a local pH-regulated PEM electrolyzer that delivered durable operation in untreated tap water for more than 3000 h at 1000 mA cm^{-2}, on par with pure-water-fed PEM systems. Local acidity provided by Brønsted acid oxides shields the membrane from cationic impurities. This local pH-regulated PEM electrolyser is projected to lower the levelized cost of hydrogen (LCOH) by 0.3–8.19%, corresponding to annual savings of roughly US$42 000–321 000.[88]

Apart from complicated impurity-induced interplay, operation at industrial-level current densities (above 500 mA cm^{-2}) with long-term durability tests (above 1000–5000 h) are often ignored in the lab-scale stage. When the best-performing sample, selected based on the lab metrics, is scaled to stack level, non-uniform gradients of physical fields, such as temperature, pressure, voltage, current density, *etc.*, would instigate system failure. This breakdown might not only be rooted in catalyst deactivation, but also in knock-on effects among device components. More seriously, the complicated real-world conditions (*e.g.*, fluctuating power input) can potentially provoke local pH changes and the alteration of the interfacial concentration of reactants or intermediates. Those intricate external factors further impose difficulties in the diagnosis of specific components.

Market-oriented research and development (R&D) further represents the golden key to unlocking the pathway toward industrial-scale implementation. Driven by clean hydrogen policies worldwide, the blueprint of market demand has been depicted as shown in Fig. 14b. In the short term, from now to 2030, the H_2 feedstock would be mainly supplied for the chemical industry, such as fertilizers and petrochemicals. According to Hydrogen Europe's strategic innovation, the goals of lowering H_2 costs to less than €3 kg^{-1} by 2030 have been established by the research agenda.[52] In the medium term, from 2030 to 2040, the extended demand for energy carriers (*e.g.*, transport and power storage) is expected to be a new growth point with more economic competitiveness than conventional energy. After 2040, aside from a wide range of application scenarios, the prosperity of the H_2 economy is anticipated to facilitate the net-zero targets by 2050.[97] Therefore, the transition from lab findings to industrial application is a complex system-level engineering challenge. Based on

impurity-induced interplay and market-oriented R&D, industrial-scale application necessitates suitable device components for stable operation under real-world conditions.

5.2. Requirements for device components

At the lab stage, tons of studies concentrate on the development of novel electrocatalysts. However, despite effective strategies as summarized in Section 3 and Table S1 (SI), assembling electrocatalysts into industrial-scale electrolysis systems is still confronted with several challenges. Micro-nano structures are subject to vigorous bubble scouring under high current densities, which may lead to material detachment. Such dynamic interfacial evolution should be fully considered when exploring strategies for performance enhancement. Interface micromechanisms obtained in simulated impure electrolytes (*e.g.*, NaCl solutions mimicking natural seawater) can hardly be extrapolated to practical conditions, because other coexisting impurities can potentially affect the active sites. More adversely, non-uniform contact interfaces, derived from the large-scale electrode fabrication process, would affect electron transport and ohmic resistance. Therefore, industrial-level evaluation should be performed from laboratory conditions to realistic environments.

Equally important as electrocatalysts, membranes are commonly used to separate the anode and cathode. However, membrane breakdown, induced by complicated impurities, poses a significant threat to the whole electrolysis system. During the long-term operation in harsh conditions, the risk of membrane swelling and fouling is remarkably enhanced, triggering the penetration of ionic impurities. In particular, ionic impurities and microorganisms present in natural seawater can markedly degrade membrane durability. The inherent defects of membranes, originating from the large-scale manufacturing process, could further induce the permeation, thereby compromising ion selectivity. Accordingly, to improve the anti-fouling and mechanical properties of membranes, it is imperative to regulate the structure of ion transport channels and the interaction of polymer chains to block impurities. More importantly, apart from modifying membrane materials, optimizing the large-scale fabrication process of advanced membranes is also essential to secure their functional performance.

To expedite the industrial application progress of DIWE, the development of electrolyzers should primarily rely on the improvements to mature technologies, such as PEMWE, AWE, and AEMWE. Analogously, design considerations regarding plate corrosion, flow fields, and reactors should be tailored for long-term operation in harsh environments. Specifically, halide ions (Cl^-, Br^-, F^-) impose destructive effects on catalysts and membranes, while also severely corroding electrolyzers. As discussed in Section 2, porous transport layers and bipolar plates, made of Ti-based materials, are susceptible to F^- corrosion in the acid medium. Moreover, *in situ*-generated impurities around the reaction microenvironment, involving metal hydroxide precipitates or detached metal catalyst particles, represent a potential threat by blocking flow channels. Concurrently, the application of other novel functional electrolyzers, as discussed in Section 4.2, is still far from large-scale commercialization, necessitating the enhancement of electrolysis efficiency and operating durability. From a long-term perspective, the current kW- or MW-scale electrolyzers are hard to exert a substantial influence on climate change, thus requiring continuous deployments to reach the TW scale.[96,287] However, the scale-up of electrolyzers and related accessories is plagued by non-uniform gradients in temperature, pressure, voltage, and current densities, *etc.* Consequently, the scale-oriented development of device components should be emphasized. Coupled with experimental validation, computer-aided numerical simulation enables the optimization of electrolyzer geometric dimensions, flow channel configurations, and physical field regulation in terms of temperature, pressure, voltage, and current density.[288]

5.3. System integration and synergistic optimization

To facilitate large-scale industrial deployment, as shown in Fig. 14c, system integration and synergistic optimization should be emphasized throughout the entire process, circumventing overemphasis on a single component or process. In particular, the Cl^--induced lattice oxygen mechanism has recently been reported for enhancing seawater oxidation reaction.[230] However, as the concentration of Cl^- goes up with continuous consumption of water, device components would inevitably be corroded during long-term operation. Despite significant performance improvements of electrocatalysts *via* this Cl^- mediated strategy, potential corrosion issues in the whole electrolysis system should not be ignored. Also, to enhance the corrosion resistance of electrodes, additional modification of electrocatalysts is usually performed in the bench-scale stage. When operating under industrial-scale conditions, some protective layers of the modified electrocatalysts are vulnerable to damage and may detach from the electrode. Those *in situ*-generated impurities pose a risk of deteriorating the membrane durability and blocking the flow channels of bipolar plates. Therefore, impurity-driven interactions do not merely occur within a single component of the device when conducting system integration. Further synergistic optimization for realizing full-chain improvement is still required to fully de-risk the DIWE technology.

A more challenging task is to strike an optimal trade-off between cost reduction and performance enhancement. Notably, electrocatalyst modification, as discussed in Section 3, usually requires an extra cost to prevent corrosion issues in harsh environments. Meanwhile, thinner membranes with reduced PFSA usage are conducive to achieving high current densities and lowering material costs.[97] However, thinner membranes are usually susceptible to degradation and possess unsatisfactory durability. Besides, the noble metal catalysts can potentially be avoided in the AWE or AEMWE system as compared to PEMWE. Conversely, PEMWE can achieve higher current densities, a rapid response time, and more integrated balance of plants. Furthermore, the cost of environmental remediation is often overlooked during the DIWE process. Due to the insufficient salt concentration in natural seawater, alkaline seawater electrolysis serves as a commonly used strategy to mitigate limited ionic conductivity. Nevertheless, the use of strong alkaline electrolytes

on offshore platforms presents substantial risks not only of the corrosion of device components but also to marine ecosystems in the event of electrolyte leakage into the ocean. Also, the salting-out effect would be intensified with the continuous consumption of water. Leaving this risk unaddressed would significantly impair environmental sustainability and long-term operational stability, thus incurring extra costs for solid and liquid waste disposal. Consequently, to identify a Pareto-optimal state enabling high-efficiency operation of electrolysis systems, trade-offs between competing factors should be carefully taken into account.

6. Conclusions and outlook

6.1. Overall review

Unlike studies centered on lab-based investigations with limited attention to market relevance, advances in the DIWE were systematically explored in this review. The merits of DIWE were first summarized as compared to the HPWE and indirect IWE technologies. Meanwhile, the potential impurity-induced challenges were introduced for a selected list of representative impurities. The easily overlooked interfacial dynamic evolution, provoked by the power fluctuations or intricate real-world conditions, was also mentioned. Based on the aforementioned challenges, more detailed reviews of the scenario-oriented electrocatalyst design and function-oriented electrolyzer development were comprehensively presented. Our analysis spans typical bottleneck issues toward cathodic precipitation and side reactions at the anode. Additionally, we underscored the threat of high-potential dissolution to the durability of catalysts. Given the abundant organic impurities existing in certain wastewater sources, the thermodynamically favorable anodic oxidation of small molecules was further emphasized to replace the sluggish OER for energy-saving. Aside from developing catalysts toward various scenarios, the conventional membrane-based electrolyzers and corresponding novel functional cell configurations were also elucidated. Ultimately, building upon our proven track record in both academia and industry, we provided systematic guidance on integrating impure water electrolysis into existing industrial workflows. What sets this review apart from others is that it delivers a multidimensional perspective, highlighting the impurity-induced interplay among components for collaboratively achieving industrial-scale DIWE.

6.2. Future outlooks

Developing DIWE exhibits immense potential to advance prospects for sustainable green hydrogen production, thereby driving a transformative shift in the global energy paradigm amid ongoing climate change. However, numerous persistent challenges remain alongside emerging opportunities, projecting our gaze towards several untapped directions. Specifically, clarifying complex interactions triggered by impurities stands as the core priority. System-level process integration and long-term durability evaluation under realistic operating conditions should be further prioritized in pilot-scale trials. Ultimately, integrated process technical packages can be established to underpin subsequent technical iteration and upgrading. Techno-economic analysis (TEA), life cycle assessment (LCA), and environmental impact assessment (EIA) are indispensable before large-scale application.[289] Collectively, achieving long-term service lifespan over 25 years under current densities exceeding 2000 mA cm^{-2} is a promising goal in the future. As illustrated in Fig. 15, standardization and conformity certification, autonomous fault diagnosis, intelligent operational maintenance, and efficient impurity utilization also provide vital supplementary directions to speed up the deployment of DIWE.

6.2.1. Standardization and conformity assessment. Despite encouraging progress, the current studies on DIWE technology involve different protocols of pre-treatments and performance evaluation, rendering it challenging to compare the performance of device components across studies. For instance, the majority of experimental data from the laboratory are acquired by using simulated seawater ($\sim$0.5 M NaCl solutions), which is vastly distinct from natural seawater with complex impurities. Meanwhile, harsh marine environments, including salt fog and UV irradiation, are commonly neglected, thereby impeding the scale-up from laboratory settings to real-world applications. Low-cost and high-efficiency pre-treatment processes are anticipated to mitigate the interference of impurities. The impact of fluctuating power input on the electrolysis system should also be comprehensively uncovered. Additionally, some studies solely rely on the comparison of the adsorption energy of key

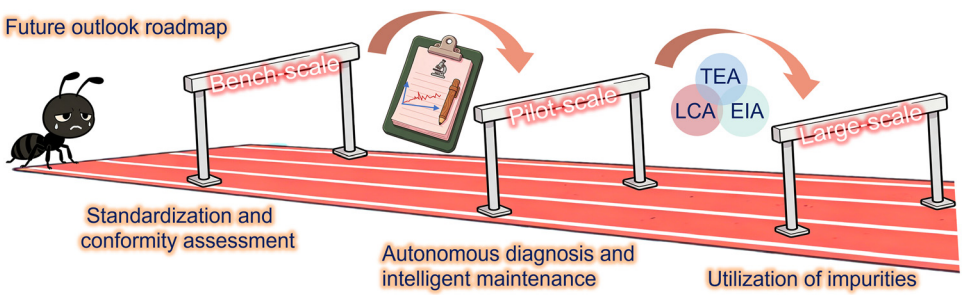

Fig. 15 Schematic illustration of the future outlook roadmap. The synergistic optimization that drives full-chain advancement from laboratory research and pilot-scale verification to large-scale industrial deployment underpins its future development. Beyond core device components, standardization and conformity evaluation, autonomous fault diagnosis, intelligent maintenance, and impurity resource utilization are also pivotal to the industrial implementation of DIWE technology.

intermediates to assess OER selectivity toward ClOR among various structural models. The dearth of solid experimental evidence from online product analysis (*e.g.*, faradaic efficiency of Cl_2 or ClO^-) precludes the establishment of high-fidelity structure-selectivity databases. Accordingly, formulating standardized protocols across the entire process, including reasonable theoretical modelling, electrolyte composition, electrolyzers, benchmark catalysts, and testing parameters, is essential for the precise and quantitative evaluation, thus facilitating the performance comparison and obtaining reliable results.

6.2.2. Autonomous diagnosis and intelligent maintenance. From the perspective of long-term operation, aspects including safety, efficiency, and reliability constitute requirements for de-risking. The system-level integration encompasses electrolysis cells and the corresponding complementary devices, such as renewable power systems, gas purification and storage systems, *etc.* When dealing with such a large system, real-time monitoring by manual intervention alone is not feasible. Therefore, operating parameters or available descriptors are needed to accurately track the simultaneous processes and interactions occurring across different scales, spanning from micro-nano scale interfacial dynamic evolution and mesoscale mass transfer to macroscale multiphysics interplay. Specifically, embracing advanced characterization techniques, such as *operando* spectroscopy and electron microscopy, creates the possibility of understanding the degradation mechanism caused by impurities around reaction microenvironments, involving morphological evolution, key intermediate adsorption–desorption, and bubble behaviors. More importantly, online product analysis plays a crucial role in detecting fluctuations in faradaic efficiency (*e.g.*, Cl_2 or ClO^-) over long-term operation. Various sensors are also indispensable for monitoring the variation of temperature and pressure, as well as unexpected pipe leakage and pump failure. Benefiting from the superior capability of deciphering complex multiparametric issues, ML is well-suited to facilitate autonomous diagnosis and intelligent maintenance. This data-driven approach relies on high-fidelity databases compiled from massive amounts of data collected during long-term operation.

6.2.3. Utilization of impurities. Driven by the imperative of cost reduction, H_2 production integrated with impurity valorization for fuels and high-value chemicals has attracted widespread research attention. Recent studies have demonstrated the efficient utilization of ionic impurities to synthesize high-value products, including the recovery of magnesium hydroxide ($Mg(OH)_2$) and chlorine gas (Cl_2), as well as the extraction of lithium (Li) and uranium (U) from seawater and wastewater.[290,291] Such promising co-production routes call for a rationally designed integrated system. Meanwhile, it is critical to optimize the energy consumption of these complex systems and improve the purity of diversified products. A commonly overlooked issue lies in the disposal of solid and liquid wastes generated during the co-production process. Furthermore, dissolved inorganic carbon and non-ionic impurities such as dissolved organic contaminants in seawater also possess great potential for recovery and reutilization.[292–294] Apart from developing strategies to mitigate the adverse effects brought by impurities, exploring their positive regulatory effects is equally vital to modulate interfacial reactions and thereby boost catalytic activity, operational stability, and reaction selectivity. In summary, although existing technologies are not yet mature enough to enable large-scale industrial deployment of DIWE, sustained research efforts and interdisciplinary collaboration among researchers and engineers will undoubtedly accelerate relevant technological innovations.

Author contributions

Jichao Zhang: He designed the overall structure of this review; wrote the original draft, prepared the abstract and introduction, and provided comprehensive revision and oversight of the entire manuscript. He communicated with groups from industry and academia. Jianrui Feng, Wei Liu, Longxiang Liu, Wei Zong, Jiexin Zhu, Ruwei Chen, Hongzhen He, Mingqiang Liu, Wei Zhang: They assisted in the drafting of Chapters 2, 3, 4, and revised relevant figures; Daojin Zhou: He assisted in writing the Introduction, Chapter 2, 3, and 4. He contributed to the overall revision, editing, and supervision. Hongtao Wang: He assisted in writing the Introduction and Chapter 5 and contributed to the overall revision, editing, and supervision. Faze Chen, Ivan P. Parkin, Xiaoming Sun, Guanjie He: They assisted in writing the Introduction and contributed to the overall revision, editing, supervision of work, as well as the finalization of the manuscript, academic verification, and communication coordination.

Conflicts of interest

There are no conflicts to declare.

Data availability

No primary research results, software or code have been included and no new data was generated or analyzed as part of this review.

Acknowledgements

The authors would like to thank the Engineering and Physical Sciences Research Council (EPSRC, EP/V027433/3), UK Research and Innovation (UKRI) under the UK Government's Horizon Europe funding (101077226; EP/Y008707/1), EPSRC Centre for Doctoral Training in Molecular Modelling and Materials Science (EP/L015862/1), and the Royal Society (RGS\R1\211080; IEC\NSFC\201261), the National Natural Science Foundation of China (22539001), the National Key Research and Development Program of China (2023YFB4005100), and the Beijing Nova Program for funding support. We also thank Huibing Liu, Dequan Fan, Yang Yang, Yanpeng Zhang, and Shengzhong Zhang from SINOPEC for their valuable insights regarding impure water electrolysis for this review.

References

1 X. Wu, J. Meng, X. Liang, L. Sun, D. Coffman, A. Kontoleon and D. Guan, *Nature*, 2025, **647**, 93–101.
2 Z. Deng, B. Zhu, S. J. Davis, P. Ciais, D. Guan, P. Gong and Z. Liu, *Nat. Rev. Earth Environ.*, 2025, **6**, 231–233.
3 J. Meckling, *Nature*, 2025, **645**, 869–876.
4 R. Chen, Y. Zhong, P. Jiang, H. Tang, F. Guo, Y. Dai, J. Chen, J. Wang, J. Liu, S. Wei, W. Zhang, W. Zong, F. Zhao, J. Zhang, Z. Guo, X. Wang and G. He, *Adv. Mater.*, 2025, **37**, 2412790.
5 X. Zou, M. Tang, Q. Lu, Y. Wang, Z. Shao and L. An, *Energy Environ. Sci.*, 2024, **17**, 386–424.
6 Y. He, W. Shang and P. Tan, *Chem. Catal.*, 2024, **4**, 101023.
7 G. Luderer, S. Madeddu, L. Merfort, F. Ueckerdt, M. Pehl, R. Pietzcker, M. Rottoli, F. Schreyer, N. Bauer, L. Baumstark, C. Bertram, A. Dirnaichner, F. Humpenöder, A. Levesque, A. Popp, R. Rodrigues, J. Strefler and E. Kriegler, *Nat. Energy*, 2021, **7**, 32–42.
8 S. An, Z.-H. Zhao, J. Bu, J. He, W. Ma, J. Lin, R. Bai, L. Shang and J. Zhang, *Angew. Chem., Int. Ed.*, 2024, **63**, e202318989.
9 J. Li, J. Lin, J. Wang, X. Lu, C. P. Nielsen, M. B. McElroy, Y. Song, J. Song, X. Lyu, M. Yu, S. Wu and Z. Yu, *Nat. Energy*, 2025, **10**, 762–773.
10 A. M. Oliveira, R. R. Beswick and Y. Yan, *Curr. Opin. Chem. Eng.*, 2021, **33**, 100701.
11 H. Tüysüz, *Acc. Chem. Res.*, 2024, **57**, 558–567.
12 S. Shiva Kumar and H. Lim, *Energy Rep.*, 2022, **8**, 13793–13813.
13 Y. Wang, Y. Xue and A. Züttel, *Chem. Soc. Rev.*, 2024, **53**, 972–1003.
14 N. Johnson, M. Liebreich, D. M. Kammen, P. Ekins, R. McKenna and I. Staffell, *Nat. Rev. Clean Technol.*, 2025, **1**, 351–371.
15 Z. Ouyang, R. B. Jackson, M. Saunois, J. G. Canadell, Y. Zhao, C. Morfopoulos, P. B. Krummel, P. K. Patra, G. P. Peters, F. Dennison, T. Gasser, A. T. Archibald, V. Arora, G. Baudoin, N. Chandra, P. Ciais, S. J. Davis, S. Feron, F. Guo, D. Hauglustaine, C. D. Jones, M. W. Jones, E. Kato, D. Kennedy, J. Knauer, S. Lienert, D. Lombardozzi, J. R. Melton, J. E. M. S. Nabel, M. O'Sullivan, G. Pétron, B. Poulter, J. Rogelj, D. Sandoval Calle, P. Smith, P. Suntharalingam, H. Tian, C. Wang and A. Wiltshire, *Nature*, 2025, **648**, 616–624.
16 Z.-Y. Yu, Y. Duan, X.-Y. Feng, X. Yu, M.-R. Gao and S.-H. Yu, *Adv. Mater.*, 2021, **33**, 2007100.
17 F. Ueckerdt, C. Bauer, A. Dirnaichner, J. Everall, R. Sacchi and G. Luderer, *Nat. Clim. Change*, 2021, **11**, 384–393.
18 O. Faye, J. Szpunar and U. Eduok, *Int. J. Hydrogen Energy*, 2022, **47**, 13771–13802.
19 M. Wappler, D. Unguder, X. Lu, H. Ohlmeyer, H. Teschke and W. Lueke, *Int. J. Hydrogen Energy*, 2022, **47**, 33551–33570.
20 Y. Li, Y. Wang, J. Wu, S. Gao, B. Zhu, J. Wang, J. Zhao, L. Wu, L. Zheng and X. Zhang, *Chem. Eng. Sci.*, 2024, **291**, 119906.
21 F. V. Maziviero, D. M. A. Melo, R. L. B. A. Medeiros, J. C. A. Silva, T. R. Araújo, Â. A. S. Oliveira, Y. K. R. O. Silva and M. A. F. Melo, *J. Energy Inst.*, 2024, **113**, 101523.
22 W. Li, J. Zhang and W. Wang, *Coord. Chem. Rev.*, 2024, **503**, 215638.
23 B. Zhang, Y. Li, R. Zhang, G. Liu, Z. Sun, B. Yang and Z. Wu, *Chem. Eng. Sci.*, 2024, **292**, 120026.
24 R. Yang, X. Che, B. Deng and Y. Lin, *Int. J. Hydrogen Energy*, 2024, **61**, 238–250.
25 S. Jiao, X. Fu, S. Wang and Y. Zhao, *Energy Environ. Sci.*, 2021, **14**, 1722–1770.
26 T. Terlouw, C. Bauer, R. McKenna and M. Mazzotti, *Energy Environ. Sci.*, 2022, **15**, 3583–3602.
27 H. Zhao and Z.-Y. Yuan, *Adv. Energy Mater.*, 2023, **13**, 2300254.
28 V. S. Thoi, Y. Sun, J. R. Long and C. J. Chang, *Chem. Soc. Rev.*, 2013, **42**, 2388–2400.
29 H. Lee, B. Choe, B. Lee, J. Gu, H.-S. Cho, W. Won and H. Lim, *J. Cleaner Prod.*, 2022, **377**, 134210.
30 D. Chen, H. Bai, J. Zhu, C. Wu, H. Zhao, D. Wu, J. Jiao, P. Ji and S. Mu, *Adv. Energy Mater.*, 2023, **13**, 2300499.
31 H. Jiang, M. Sun, S. Wu, B. Huang, C.-S. Lee and W. Zhang, *Adv. Funct. Mater.*, 2021, **31**, 2104951.
32 M. Wang, H. Dai and Q. Yang, *Angew. Chem., Int. Ed.*, 2023, **62**, e202309929.
33 S. Zhang, P. Zhao, F. Wang, H. Basma, F. Rodriguez, T. J. Wallington, G. A. Keoleian and Y. Wu, *Nat. Rev. Clean Technol.*, 2025, **1**, 846–860.
34 A. Devlin, J. Kossen, H. Goldie-Jones and A. Yang, *Nat. Commun.*, 2023, **14**, 2578.
35 F. B. Juangsa, A. S. Cezeliano, P. S. Darmanto and M. Aziz, *S. Afr. J. Chem. Eng.*, 2022, **42**, 23–31.
36 N. Guruprasad, J. Van Der Schaaf and M. T. De Groot, *J. Power Sources*, 2024, **613**, 234877.
37 C. Rong, Q. Meyer, H. Lu and C. Zhao, *Adv. Mater.*, 2025, **38**, e12414.
38 E. Uwadiunor, V. Kotasthane, D. K. Yesudoss, H. Nguyen, E. Pranada, K. Obodo, M. Radovic and A. Djire, *Chem. Catal.*, 2023, **3**, 100634.
39 N. Dubouis, D. Aymé-Perrot, D. Degoulange, A. Grimaud and H. Girault, *Joule*, 2024, **8**, 883–898.
40 J. Wang, J. Yang, Y. Feng, J. Hua, Z. Chen, M. Liao, J. Zhang and J. Qin, *Appl. Energy*, 2025, **379**, 124936.
41 W. Musie and G. Gonfa, *Heliyon*, 2023, **9**, e18685.
42 L. Wu, Y. Xu, Q. Wang, X. Zou, Z. Pan, M. K. H. Leung and L. An, *Energy Environ. Sci.*, 2025, **18**, 4596–4624.
43 A. Getirana, N. Kumar Biswas, S. Kumar, W. Nie, S. Ahmad, F. Maina, N. Sakib, M. S. Hossain and R. K. Biswas, *Nat. Sustainability*, 2025, **8**, 914–924.
44 S. Hou, J. Huo, X. Zhao, X. Wang, X. Zhang, D. Zhao, M. R. Tillotson, Y. Shan, M. Flörke, W. Guo, J. Meng and K. Hubacek, *Nat. Water*, 2025, **3**, 439–448.
45 R. Jiang, H. Lu, D. Chen, K. Yang, D. Guan, G. Huang and F. Tian, *Nat. Commun.*, 2025, **16**, 8166.
46 D. Macias, B. Bisselink, C. Carmona-Moreno, J.-N. Druon, O. Duteil, E. Garcia-Gorriz, B. Grizzetti, J. Guillen,

S. Miladinova, A. Pistocchi, C. Piroddi, L. Polimene, N. Serpetti, A. Stips, I. Trichakis, A. Udias and O. Vigiak, *Nat. Commun.*, 2025, **16**, 998–1009.
47 H. Le, K. Key, M. S. Steckler, N. Sazeed, M. Person, A. Bhuiyan, M. R. Khan and K. M. Ahmed, *Nat. Commun.*, 2025, **16**, 10740.
48 C. Govoni, L. Zhuo, D. M. Marchioni and M. C. Rulli, *Nat. Food*, 2025, **6**, 954–967.
49 V. P. Ravinandrasana and C. L. E. Franzke, *Nat. Commun.*, 2025, **16**, 8281.
50 Y. Wang, F. Ma, H. Wang, A. Tzachor, M. Jiang, K. Fang, S. Liang, B. Zhu, E. G. Hertwich, M. Lenzen, H. Schandl and S. Lutter, *Nat. Sustainability*, 2025, **8**, 1554–1566.
51 R. Prieto-Curiel, P. Luengas-Sierra and C. Borja-Vega, *Nat. Cities*, 2025, **2**, 1148–1159.
52 H. Becker, J. Murawski, D. V. Shinde, I. E. L. Stephens, G. Hinds and G. Smith, *Sustainable Energy Fuels*, 2023, **7**, 1565–1603.
53 S. Ten Hietbrink, H. Patton, B. Dugan, B. Szymczycha, A. Sen, A. Lepland, J. Knies, J.-H. Kim, N.-C. Chen and W.-L. Hong, *Nat. Geosci.*, 2025, **18**, 779–786.
54 R.-T. Gao, Z. Gao, N. T. Nguyen, J. Chen, X. Liu, L. Wang and L. Wu, *Nat. Sustainability*, 2025, **8**, 672–681.
55 A. Robertson, W. Musial, M. Shields, A. Aubault, M. Ikari and L. Kitzing, *Nat. Rev. Clean Technol.*, 2025, **1**, 734–749.
56 F. W. Geels and A. D. Andersen, *Nat. Sustainability*, 2026, **9**, 501–508.
57 C. Smith and L. Torrente-Murciano, *Nat. Chem. Eng.*, 2025, **2**, 261–272.
58 D. Navia Simon and L. Diaz Anadon, *Nat. Energy*, 2025, **10**, 329–341.
59 B. Ouyang, R. Huang, P. Chen, T. Zhang, D. Wei, H. Dong, Y. Qing, Y. He, W. Zhang, H. Wang and L. Chai, *Angew. Chem., Int. Ed.*, 2025, **138**, e22623.
60 X. Jiang, C. Li, Y. Chen, J. Chen, Z. Guo, Q. Zhou, L. Zhu, D. Lin and J. Xu, *Nat. Water*, 2026, **4**, 206–216.
61 J. Li, J. W. O'Brien, B. J. Tscharke, C. He, K. M. Shimko, X. Shao, N. Zhai, J. F. Mueller and K. V. Thomas, *Nat. Water*, 2024, **2**, 1166–1177.
62 Q. Wu, S. Ji, J. Chen, X.-Q. Tan, W.-J. Ong, R. Du, P. Wang, H. Wang, Y. Qiu, K. Yan, Y. Zhao, W.-W. Zhao, K.-S. Peng, Y.-Y. Chen, S.-F. Hung, L. Zhou, X. Wang, G. Qiu and G. Chen, *Nat. Water*, 2025, **3**, 1291–1302.
63 A. Christou, V. G. Beretsou, I. C. Iakovides, P. Karaolia, C. Michael, T. Benmarhnia, B. Chefetz, E. Donner, B. M. Gawlik, Y. Lee, T. T. Lim, L. Lundy, R. Maffettone, L. Rizzo, E. Topp and D. Fatta-Kassinos, *Nat. Rev. Earth Environ.*, 2024, **5**, 504–521.
64 J. Zhu, X. Hu, J. Feng, H. He, X. Gao, Z. Lin, H. Dong, G. He and I. P. Parkin, *Cell Rep. Phys. Sci.*, 2026, **7**, 103045.
65 Y. Zhao, Y. Zhang, Y. Wei, J. Chen, L. Fan, J. Chen, S. Xi, M. Luo, L. Shen and L. Wang, *Chem Catal.*, 2026, **6**, 101573.
66 J.-T. Ren, L. Chen and Z.-Y. Yuan, *Mater. Today*, 2025, **86**, 282–316.
67 F.-Y. Gao, P.-C. Yu and M.-R. Gao, *Curr. Opin. Chem. Eng.*, 2022, **36**, 100827.
68 R. Lu, B. Wang, L. Li, Z. Bao, B. Li, Q. Du and K. Jiao, *Sci. Bull.*, 2026, **71**, 172–195.
69 L. Huang, D. Bao, Y. Jiang, K. Regenauer-Lieb, Y. Zheng and S.-Z. Qiao, *Natl. Sci. Rev.*, 2025, **12**, nwaf461.
70 X. Hu, S. Cheng, U. Farooq, I. Ul Islam and X. Wang, *Angew. Chem., Int. Ed.*, 2025, **64**, e202505094.
71 B. Liu, C. Yang, X. Huang, Y. Pan, C. Cheng, W. Guo, L. Liang, Z. Wang and F. He, *Nat. Commun.*, 2025, **16**, 10963.
72 J. Zhang, J. Zhu, L. Kang, Q. Zhang, L. Liu, F. Guo, K. Li, J. Feng, L. Xia, L. Lv, W. Zong, P. R. Shearing, D. J. L. Brett, I. P. Parkin, X. Song, L. Mai and G. He, *Energy Environ. Sci.*, 2023, **16**, 6015–6025.
73 J. Zhang, X. Song, L. Kang, J. Zhu, L. Liu, Q. Zhang, D. J. L. Brett, P. R. Shearing, L. Mai, I. P. Parkin and G. He, *Chem Catal.*, 2022, **2**, 3254–3270.
74 F. Ribalet, S. Dutkiewicz, E. Monier and E. V. Armbrust, *Nat. Microbiol.*, 2025, **10**, 2441–2453.
75 X. Cao, S. Chen, Y. Liu, G. Long and Y. J. Xu, *Nat. Commun.*, 2025, **16**, 7522.
76 S. Zhang, P. Li, Q. Hu, Y. Xue, Y. Wu, H. Huang, Y.-X. Zhang, Z. Ya, T. Tan, J. Liu and Z. Niu, *Adv. Mater.*, 2025, **37**, e08428.
77 X. Sun, R. B. Araujo, E. C. Dos Santos, Y. Sang, H. Liu and X. Yu, *Chem. Soc. Rev.*, 2024, **53**, 7392–7425.
78 Y. Wang, Z. Shi, M. Luo, Y. Zhai, C. Jing, L. Ding, S. Dai, K.-G. Zhou, L. Li, S. Li, J. Luo, Y. Zhao, W. Wu, Z. Lu, L. Lan, W. Li, Y. Wei and H. Wang, *Nat. Commun.*, 2025, **16**, 10005.
79 S. Yu, Y. Chen, Z. Qiao and J. Hou, *Chem. Soc. Rev.*, 2026, **55**, 2229–2264.
80 K. Qi, L. Gao, X. Li and F. He, *Catalysts*, 2023, **13**, 855.
81 M. G. O'Connell, N. Rajendran, M. Elimelech, J. Gilron and J. B. Dunn, *Nat. Water*, 2024, **2**, 1116–1127.
82 H. Liu, X. Sun, F.-Y. Gao, Y. Zheng and S.-Z. Qiao, *Nat. Catal.*, 2026, **9**, 9–17.
83 S. Zhao, C. Jiang, J. Fan, S. Hong, P. Mei, R. Yao, Y. Liu, S. Zhang, H. Li, H. Zhang, C. Sun, Z. Guo, P. Shao, Y. Zhu, J. Zhang, L. Guo, Y. Ma, J. Zhang, X. Feng, F. Wang, H. Wu and B. Wang, *Nat. Mater.*, 2021, **20**, 1551–1558.
84 J. Zhao, Y. Zhang, Y. Ye, Q. Xu, S. Luo, F. Meng, S. Zhu, X. Li, X. Lin, A. Yu, X. Ren, T. Wu and Z. J. Xu, *Nat. Commun.*, 2025, **16**, 5601.
85 J. Zhang, X. Fu, S. Kwon, K. Chen, X. Liu, J. Yang, H. Sun, Y. Wang, T. Uchiyama, Y. Uchimoto, S. Li, Y. Li, X. Fan, G. Chen, F. Xia, J. Wu, Y. Li, Q. Yue, L. Qiao, D. Su, H. Zhou, W. A. Goddard and Y. Kang, *Science*, 2025, **387**, 48–55.
86 R. Ram, L. Xia, H. Benzidi, A. Guha, V. Golovanova, A. Garzón Manjón, D. Llorens Rauret, P. Sanz Berman, M. Dimitropoulos, B. Mundet, E. Pastor, V. Celorrio, C. A. Mesa, A. M. Das, A. Pinilla-Sánchez, S. Giménez, J. Arbiol, N. López and F. P. García de Arquer, *Science*, 2024, **384**, 1373–1380.
87 Y. Zhao, P. Yin, Y. Yang, R. Wang, C. Gong, J. Li, J. Guo, Q. Wang and T. Ling, *Angew. Chem., Int. Ed.*, 2025, **64**, e202419501.

88 R. Wang, Y. Yang, J. Guo, Q. Zhang, F. Cao, Y. Wang, L. Han and T. Ling, *Nat. Energy*, 2025, **10**, 880–889.
89 J. Guo, Y. Zheng, Z. Hu, C. Zheng, J. Mao, K. Du, M. Jaroniec, S.-Z. Qiao and T. Ling, *Nat. Energy*, 2023, **8**, 264–272.
90 L. Yu, M. Ning, Y. Wang, C. Yuan and Z. Ren, *Nat. Rev. Mater.*, 2025, **10**, 857–873.
91 S. Park, Y. H. Lee, S. Choi, H. Seo, M. Y. Lee, M. Balamurugan and K. T. Nam, *Energy Environ. Sci.*, 2020, **13**, 2310–2340.
92 Z. Zhou, Z. Pei, L. Wei, S. Zhao, X. Jian and Y. Chen, *Energy Environ. Sci.*, 2020, **13**, 3185–3206.
93 J. Yu, B.-Q. Li, C.-X. Zhao and Q. Zhang, *Energy Environ. Sci.*, 2020, **13**, 3253–3268.
94 J. Huang, B. Hu, J. Meng, T. Meng, W. Liu, Y. Guan, L. Jin and X. Zhang, *Energy Environ. Sci.*, 2024, **17**, 1007–1045.
95 L. Wu, Q. Wang, W. Li, M. Tang and L. An, *Mater. Rep.: Energy*, 2025, **5**, 100356.
96 M. A. Riaz, P. Trogadas, D. Aymé-Perrot, C. Sachs, N. Dubouis, H. Girault and M.-O. Coppens, *Energy Environ. Sci.*, 2025, **18**, 5190–5214.
97 A. Karl, E. Jodat, H. Kungl, L. Dobrenizki, G. Schmid, P. Geskes and R.-A. Eichel, *Electrochem. Sci. Adv.*, 2025, **5**, e202400041.
98 World enters era of 'global water bankruptcy' | UN news, https://news.un.org/en/story/2026/01/1166800, (accessed January 22, 2026).
99 C. R. Wang, J. M. Stansberry, R. Mukundan, H.-M. J. Chang, D. Kulkarni, A. M. Park, A. B. Plymill, N. M. Firas, C. P. Liu, J. T. Lang, J. K. Lee, N. E. Tolouei, Y. Morimoto, C. Wang, G. Zhu, J. Brouwer, P. Atanassov, C. B. Capuano, C. Mittelsteadt, X. Peng and I. V. Zenyuk, *Chem. Rev.*, 2025, **125**, 1257–1302.
100 G. A. Lindquist, Q. Xu, S. Z. Oener and S. W. Boettcher, *Joule*, 2020, **4**, 2549–2561.
101 H. Qazi, D. Chauhan and Y.-H. Ahn, *Int. J. Hydrogen Energy*, 2025, **99**, 155–164.
102 M. Carmo, D. L. Fritz, J. Mergel and D. Stolten, *Int. J. Hydrogen Energy*, 2013, **38**, 4901–4934.
103 M. A. Khan, T. Al-Attas, S. Roy, M. M. Rahman, N. Ghaffour, V. Thangadurai, S. Larter, J. Hu, P. M. Ajayan and M. G. Kibria, *Energy Environ. Sci.*, 2021, **14**, 4831–4839.
104 J. Lei, H. Zhang, J. Pan, Y. Zhuo, A. Chen, W. Chen, Z. Yang, K. Feng, L. Li, B. Wang, L. Jiao and K. Jiao, *Energies*, 2024, **17**, 2447.
105 X. Liu, S. Shanbhag, T. V. Bartholomew, J. F. Whitacre and M. S. Mauter, *ACS ES&T Eng.*, 2021, **1**, 261–273.
106 S. He, T. Zhu, Y. Wang, W. Xiong, X. Gao and E. Zhang, *Environ. Sci.: Water Res. Technol.*, 2024, **10**, 2313–2340.
107 M. Tauk, G. Folaranmi, M. Cretin, M. Bechelany, P. Sistat, C. Zhang and F. Zaviska, *J. Environ. Chem. Eng.*, 2023, **11**, 111368.
108 J. N. Hausmann, L. R. Winter, M. A. Khan, M. Elimelech, M. G. Kibria, T. Sontheimer and P. W. Menezes, *Joule*, 2024, **8**, 2436–2442.
109 J. Liang, Z. Cai, Z. Li, Y. Yao, Y. Luo, S. Sun, D. Zheng, Q. Liu, X. Sun and B. Tang, *Nat. Commun.*, 2024, **15**, 2950.
110 X. He, Y. Yao, L. Zhang, H. Wang, H. Tang, W. Jiang, Y. Ren, J. Nan, Y. Luo, T. Wu, F. Luo, B. Tang and X. Sun, *Nat. Commun.*, 2025, **16**, 4998.
111 L. Yi, C. Chen, Y. Wen, S. Zhang, H. Chen, J. Zhu, J. Weng, W. Zhang, W. Xu, W. Guan, X. Chen, T. Qiu, X. Tian and Z. Lu, *Nat. Commun.*, 2025, **16**, 11493.
112 Q. Sha, S. Wang, L. Yan, Y. Feng, Z. Zhang, S. Li, X. Guo, T. Li, H. Li, Z. Zhuang, D. Zhou, B. Liu and X. Sun, *Nature*, 2025, **639**, 360–367.
113 T. Liu, Z. Zhao, W. Tang, Y. Chen, C. Lan, L. Zhu, W. Jiang, Y. Wu, Y. Wang, Z. Yang, D. Yang, Q. Wang, L. Luo, T. Liu and H. Xie, *Nat. Commun.*, 2024, **15**, 5305.
114 Z. Zhu, S. Ma, H. Mao, J. Zhong, L. Guo, D. Wang, J. Huang, C. Miao, X. Zhang, X. Zhang and D. Zhang, *Appl. Energy*, 2025, **398**, 126413.
115 O. Schmidt, A. Gambhir, I. Staffell, A. Hawkes, J. Nelson and S. Few, *Int. J. Hydrogen Energy*, 2017, **42**, 30470–30492.
116 J. Brauns and T. Turek, *Processes*, 2020, **8**, 248.
117 S. Barwe, B. Mei, J. Masa, W. Schuhmann and E. Ventosa, *Nano Energy*, 2018, **53**, 763–768.
118 Y. Jin, P. Behrens, A. Tukker and L. Scherer, *Renew. Sustain. Energy Rev.*, 2019, **115**, 109391.
119 L. Du, J. Jiang, G. Zhou, Y. Yan, R. S. Kingsbury, A. Y. Ku and Z. J. Ren, *Water Res.*, 2026, **288**, 124672.
120 R. Yuan, C. Liao, L. Cao, D. Li, S. Sun, G. Wang, G. Li, J. Xie and Z. Shao, *Adv. Funct. Mater.*, 2026, **36**, e08413.
121 L. Wu, W. L. Ong and G. W. Ho, *ACS Nano*, 2025, **19**, 10779–10795.
122 R. Wang, K. Yang, C. Wong, H. Aguirre-Villegas, R. Larson, F. Brushett, M. Qin and S. Jin, *Nat. Sustainability*, 2023, **7**, 179–190.
123 M. Farghali, Z. Chen, A. I. Osman, I. M. Ali, D. Hassan, I. Ihara, D. W. Rooney and P.-S. Yap, *Environ. Chem. Lett.*, 2024, **22**, 2699–2751.
124 L. Babcock-Jackson, T. Konovalova, J. P. Krogman, R. Bird and L. L. Díaz, *J. Agric. Food Chem.*, 2023, **71**, 8265–8296.
125 S. Vaishnav, T. Saini, A. Chauhan, G. K. Gaur, R. Tiwari, T. Dutt and A. Tarafdar, *Bioresour. Technol.*, 2023, **382**, 129170.
126 C. Hou, H. Wu, Z. Zhou, S. Peng, K. Wu, Y. Wang, L. Xu, Z. Chen, Z. Lei and D. Wu, *Water Res.*, 2025, **268**, 122589.
127 G. Qu, Z. Yuan, C. Zhao, G. Liu, K. Xiang, Y. Yang and J. Li, *Waste Biomass Valorization*, 2025, **16**, 1015–1043.
128 W. Xiong, M. Yang, J. Wang, H. Wang, P. Zhao, Z. Li, B. Liu, X. Kong, H. Duan and Y. Zhao, *Chem. Eng. Sci.*, 2023, **279**, 118928.
129 P. Sahu, A. R. Patel, A. Pandey, M. Hait and G. K. Patra, *Inorg. Chim. Acta*, 2025, **585**, 122751.
130 T. E. Oladimeji, M. Oyedemi, M. E. Emetere, O. Agboola, J. B. Adeoye and O. A. Odunlami, *Heliyon*, 2024, **10**, e40370.
131 N. A. A. Qasem, R. H. Mohammed and D. U. Lawal, *npj Clean Water*, 2021, **4**, 36.
132 S. Rajoria, M. Vashishtha and V. K. Sangal, *Chem. Eng. Process Tech*, 2023, **8**, 1082.
133 T. Lim, H. Ooka, Y. Yu, T. Murakami, S. Wada and R. Nakamura, *Nat. Chem.*, 2025, **18**, 552–560.

134 J. Zaffran, M. B. Stevens, C. D. M. Trang, M. Nagli, M. Shehadeh, S. W. Boettcher and M. Caspary Toroker, *Chem. Mater.*, 2017, **29**, 4761–4767.
135 M. Maril, J.-L. Delplancke, C. Salvo, S. Hevia, T. Alvear and C. Carrasco, *J. Electroanal. Chem.*, 2024, **967**, 118422.
136 E. C. La Plante, X. Chen, S. Bustillos, A. Bouissonnie, T. Traynor, D. Jassby, L. Corsini, D. A. Simonetti and G. N. Sant, *ACS ES&T Eng.*, 2023, **3**, 955–968.
137 S. Feng, Y. Yu, C. Wang, P. Ling, T. Wang, W. Shi, J. Li, X. Han, D. Wu, Z. Kang, Y. Yuan and X. Tian, *Chem Catal.*, 2025, **5**, 101551.
138 H. Hu, X. Wang, J. P. Attfield and M. Yang, *Chem. Soc. Rev.*, 2024, **53**, 163–203.
139 A. Malek, Y. Xue and X. Lu, *Angew. Chem., Int. Ed.*, 2023, **62**, e202309854.
140 Z. Li, Y. Yao, S. Sun, J. Liang, S. Hong, H. Zhang, C. Yang, X. Zhang, Z. Cai, J. Li, Y. Ren, Y. Luo, D. Zheng, X. He, Q. Liu, Y. Wang, F. Gong, X. Sun and B. Tang, *Angew. Chem., Int. Ed.*, 2024, **63**, e202316522.
141 Y. Kuang, M. J. Kenney, Y. Meng, W.-H. Hung, Y. Liu, J. E. Huang, R. Prasanna, P. Li, Y. Li, L. Wang, M.-C. Lin, M. D. McGehee, X. Sun and H. Dai, *Proc. Natl. Acad. Sci. U. S. A.*, 2019, **116**, 6624–6629.
142 X.-L. Zhang, P.-C. Yu, S.-P. Sun, L. Shi, P.-P. Yang, Z.-Z. Wu, L.-P. Chi, Y.-R. Zheng and M.-R. Gao, *Nat. Commun.*, 2024, **15**, 9462.
143 K. Hongsirikarn, J. G. Goodwin, S. Greenway and S. Creager, *J. Power Sources*, 2010, **195**, 30–38.
144 K. Hongsirikarn, T. Napapruekchart, X. Mo and J. G. Goodwin, *J. Power Sources*, 2011, **196**, 644–651.
145 R. Kuwertz, C. Kirstein, T. Turek and U. Kunz, *J. Membr. Sci.*, 2016, **500**, 225–235.
146 M. B. Stevens, C. D. M. Trang, L. J. Enman, J. Deng and S. W. Boettcher, *J. Am. Chem. Soc.*, 2017, **139**, 11361–11364.
147 K. Kawashima, R. A. Márquez-Montes, H. Li, K. Shin, C. L. Cao, K. M. Vo, Y. J. Son, B. R. Wygant, A. Chunangad, D. H. Youn, G. Henkelman, V. H. Ramos-Sánchez and C. B. Mullins, *Mater. Adv.*, 2021, **2**, 2299–2309.
148 A. Kusoglu and A. Z. Weber, *Chem. Rev.*, 2017, **117**, 987–1104.
149 Y. Zhang, G. Guo, H. Wu, Y. Mu, P. Liu, J. Liu and C. Zhang, *Sci. Total Environ.*, 2019, **692**, 82–88.
150 N. Ahmad, M. Usman, H. R. Ahmad, M. Sabir, Z. U. R. Farooqi and M. T. Shehzad, *Environ. Monit. Assess.*, 2023, **195**, 1326.
151 G. He, L. Zhao, K. Chen, Y. Liu and H. Zhu, *Talanta*, 2013, **106**, 73–78.
152 H. Amar, M. Benzaazoua, A. Elghali, R. Hakkou and Y. Taha, *J. Cleaner Prod.*, 2022, **381**, 135151.
153 Z. Xu, Z. Chen, S. Peng, S. Bai, X. Li, G. Wang, R. Zheng and B.-J. Ni, *J. Environ. Chem. Eng.*, 2025, **13**, 117695.
154 Z. Xu, Y. Zhang, N. J. D. Graham, S. J. Parikh, X. Xu, X. Cao, Y. S. Ok, S. M. Shaheen, J. Rinklebe and D. C. W. Tsang, *Commun. Mater.*, 2025, **6**, 47–56.
155 A. Di Corcia, L. Capuani, F. Casassa, A. Marcomini and R. Samperi, *Environ. Sci. Technol.*, 1999, **33**, 4119–4125.
156 H. Eslami, M. R. Samaei, E. Shahsavani and A. A. Ebrahimi, *Desalin. Water Treat.*, 2017, **92**, 128–133.
157 Y. Luo, X. Jin, H. Xie, X. Ji, Y. Liu, C. Guo, J. P. Giesy and J. Xu, *J. Environ. Manage.*, 2023, **342**, 118344.
158 S. Dresp, T. N. Thanh, M. Klingenhof, S. Brückner, P. Hauke and P. Strasser, *Energy Environ. Sci.*, 2020, **13**, 1725–1729.
159 S. Zhang, Y. Wang, S. Li, Z. Wang, H. Chen, L. Yi, X. Chen, Q. Yang, W. Xu, A. Wang and Z. Lu, *Nat. Commun.*, 2023, **14**, 4822.
160 W. Tong, M. Forster, F. Dionigi, S. Dresp, R. Sadeghi Erami, P. Strasser, A. J. Cowan and P. Farràs, *Nat. Energy*, 2020, **5**, 367–377.
161 T. Ma, W. Xu, B. Li, X. Chen, J. Zhao, S. Wan, K. Jiang, S. Zhang, Z. Wang, Z. Tian, Z. Lu and L. Chen, *Angew. Chem., Int. Ed.*, 2021, **60**, 22740–22744.
162 F. Gossenberger, F. Juarez and A. Groß, *Front. Chem.*, 2020, **8**, 634.
163 A. Kolics and A. Wieckowski, *J. Phys. Chem. B*, 2001, **105**, 2588–2595.
164 A. Ganassin, V. Colic, J. Tymoczko, A. S. Bandarenka and W. Schuhmann, *Phys. Chem. Chem. Phys.*, 2015, **17**, 8349–8355.
165 X. Sun, W. Shen, H. Liu, P. Xi, M. Jaroniec, Y. Zheng and S.-Z. Qiao, *Nat. Commun.*, 2024, **15**, 10351.
166 R. Fan, C. Liu, Z. Li, H. Huang, J. Feng, Z. Li and Z. Zou, *Nat. Sustainability*, 2024, **7**, 158–167.
167 W. Liu, J. Yu, M. G. Sendeku, T. Li, W. Gao, G. Yang, Y. Kuang and X. Sun, *Angew. Chem., Int. Ed.*, 2023, **62**, e202309882.
168 H. Liao, T. Luo, P. Tan, K. Chen, L. Lu, Y. Liu, M. Liu and J. Pan, *Adv. Funct. Mater.*, 2021, **31**, 2102772.
169 Y. Yu, W. Zhou, J. Yuan, X. Zhou, X. Meng, X. Zhang, X. Li, N. Xue, Y. Chen, X. Xia, M. Gu, J. Chen, X. Wang, F. Sun, J. Gao and G. Zhao, *Energy Environ. Sci.*, 2025, **18**, 9949–9958.
170 J. Cheng, W. Liu, S. Chen, Y. Zhang, A. Cao, Y. Zhang, Z. Shen, Y. Yang, Y. Zhang, Y. Li, D. Zhou and X. Sun, *Angew. Chem., Int. Ed.*, 2025, **64**, e18106.
171 N. T. Thomas and K. Nobe, *J. Electrochem. Soc.*, 1969, **116**, 1748.
172 Z. B. Wang, H. X. Hu, C. B. Liu and Y. G. Zheng, *Electrochim. Acta*, 2014, **135**, 526–535.
173 D.-S. Kong and Y.-Y. Feng, *J. Electrochem. Soc.*, 2009, **156**, C283.
174 D.-S. Kong, *Langmuir*, 2008, **24**, 5324–5331.
175 A. Onal, I. Kahveci and M. Soylak, *Asian J. Chem.*, 2004, **16**, 445–452.
176 M. Seyedsalehi, O. Paladino, G. Hodaifa, M. Sillanpää, K. Gurung, M. Sahafnia and H. Barzanouni, *Int. J. Environ. Sci. Technol.*, 2019, **16**, 6763–6772.
177 Y. Tan, J. Feng, L. Kang, L. Liu, F. Zhao, S. Zhao, D. J. L. Brett, P. R. Shearing, G. He and I. P. Parkin, *Energy Environ. Mater.*, 2023, **6**, e12398.
178 Z. Su, Z. Dai, C. Zhou, L. Li, T. Zhou, Z. Man, Y. Wang, Y. Chen, C. Xie, J. Li, J. Bai and B. Zhou, *Appl. Catal., B*, 2025, **375**, 125419.

179 T. Smolinka, M. Heinen, Y. X. Chen, Z. Jusys, W. Lehnert and R. J. Behm, *Electrochim. Acta*, 2005, **50**, 5189–5199.
180 Y. Li and C. Ning, *Bioact. Mater.*, 2019, **4**, 189–195.
181 D. M. Yebra, S. Kiil and K. Dam-Johansen, *Prog. Org. Coat.*, 2004, **50**, 75–104.
182 H. Jin, J. Wang, L. Tian, M. Gao, J. Zhao and L. Ren, *Mater. Des.*, 2022, **213**, 110307.
183 M. Maril, J.-L. Delplancke, N. Cisternas, P. Tobosque, Y. Maril and C. Carrasco, *Int. J. Hydrogen Energy*, 2022, **47**, 3532–3549.
184 H. Kojima, K. Nagasawa, N. Todoroki, Y. Ito, T. Matsui and R. Nakajima, *Int. J. Hydrogen Energy*, 2023, **48**, 4572–4593.
185 Q. Hassan, A. Z. Sameen, H. M. Salman and M. Jaszczur, *Energy Harvesting Syst.*, 2024, **11**, 20230011.
186 A. Li, H. Ooka, S. Kong, K. Adachi, Y. Zhang, K. Fushimi, S. Hamamoto, M. Oura, S. H. Kim, D. Hashizume and R. Nakamura, *Nat. Sustainability*, 2025, **8**, 1533–1540.
187 W. Liu, J. Yu, B. Ding, T. Li, S. Li, X. Guo, L. Zhou, B. Tian, Y. Zhang, Y. Li, M. Ma, K. Wang, H. Xin, D. Zhou, Y. Kuang and X. Sun, *Nano Res.*, 2025, **18**, 94907246.
188 W.-G. Cui, F. Gao, G. Na, X. Wang, Z. Li, Y. Yang, Z. Niu, Y. Qu, D. Wang and H. Pan, *Chem. Soc. Rev.*, 2024, **53**, 10253–10311.
189 L. Xia, B. F. Gomes, W. Jiang, D. Escalera-López, Y. Wang, Y. Hu, A. Y. Faid, K. Wang, T. Chen, K. Zhao, X. Zhang, Y. Zhou, R. Ram, B. Polesso, A. Guha, J. Su, C. M. S. Lobo, M. Haumann, R. Spatschek, S. Sunde, L. Gan, M. Huang, X. Zhou, C. Roth, W. Lehnert, S. Cherevko, L. Gan, F. P. García De Arquer and M. Shviro, *Nat. Mater.*, 2025, **24**, 753–761.
190 Z.-P. Wu, S. Zuo, Z. Pei, J. Zhang, L. Zheng, D. Luan, H. Zhang and X. W. (David) Lou, *Sci. Adv.*, 2025, **11**, eadu5370.
191 J.-W. Zhao, Y. Li, D. Luan and X. W. (David) Lou, *Sci. Adv.*, 2024, **10**, eadq4696.
192 J. Feng, X. Wang and H. Pan, *Adv. Mater.*, 2024, **36**, 2411688.
193 Q. Xu, J. Zhang, H. Zhang, L. Zhang, L. Chen, Y. Hu, H. Jiang and C. Li, *Energy Environ. Sci.*, 2021, **14**, 5228–5259.
194 J. Zhang, J. Dang, X. Zhu, J. Ma, M. Ouyang and F. Yang, *Appl. Catal., B*, 2023, **325**, 122296.
195 X. Zou and Y. Zhang, *Chem. Soc. Rev.*, 2015, **44**, 5148–5180.
196 L. Zhao, S. Zhou, Z. Lv, W. Xu, J. Liu, Z. Liu, Q. Zhang, J. Lai and L. Wang, *Appl. Catal., B*, 2023, **338**, 122996.
197 D. Bao, L. Huang, Y. Gao, K. Davey, Y. Zheng and S.-Z. Qiao, *J. Am. Chem. Soc.*, 2024, **146**, 34711–34719.
198 L. Yi, X. Chen, Y. Wen, H. Chen, S. Zhang, H. Yang, W. Li, L. Zhou, B. Xu, W. Xu, W. Guan, S. Dai and Z. Lu, *Nano Lett.*, 2024, **24**, 5920–5928.
199 Y. Zhu, W. Duan, Z. Huang, L. Tian, W. Wu, Z. Dang and C. Feng, *Environ. Sci. Technol.*, 2024, **58**, 13145–13156.
200 L. Ventimiglia, F. Vassallo, G. Lo Burgio, A. Campione, L. Cammilli, P. Vicario, G. Battaglia, F. Vicari, A. Cipollina, A. Tamburini and G. Micale, *Desalination*, 2025, **613**, 119052.
201 J. Tang, Q. Zeng, Q. Jiang, H. Wang, S. Hu, Y. Ji, H. Zeng, C. Liu, H.-J. Peng, X. Li, T. Zheng, C.-W. Pao, X. Liu and C. Xia, *Chem. Catal.*, 2025, **5**, 101441.
202 F. Dionigi, T. Reier, Z. Pawolek, M. Gliech and P. Strasser, *ChemSusChem*, 2016, **9**, 962–972.
203 A. G. Rajan and E. A. Carter, *Energy Environ. Sci.*, 2020, **13**, 4962–4976.
204 T. Liu, Z. Zhao, W. Tang, Y. Wu, C. Lan, W. Jiang and H. Xie, *Nat. Rev. Clean Technol.*, 2026, **2**, 305–319.
205 V. H. Hoa, M. Austeria, H. Thi Dao, M. Mai and D. H. Kim, *Appl. Catal., B*, 2023, **327**, 122467.
206 P. Tian, W. Zong, J. Xiong, W. Liu, J. Liu, Y. Dai, J. Zhu, S. Huang, S. Song, K. Chu, G. He and N. Han, *Adv. Funct. Mater.*, 2025, **35**, 2504862.
207 P. Lu, J. Huo, M. Cui, Y. Dou, W. Li, H.-K. Liu, Z. Bai, S.-X. Dou and R. Ge, *Adv. Funct. Mater.*, 2025, **36**, e16798.
208 Y. Yu, W. Zhou, X. Zhou, J. Yuan, X. Zhang, X. Meng, F. Sun, J. Gao and G. Zhao, *Adv. Funct. Mater.*, 2025, **35**, 2419871.
209 C. Huang, Q. Zhou, D. Duan, L. Yu, W. Zhang, Z. Wang, J. Liu, B. Peng, P. An, J. Zhang, L. Li, J. Yu and Y. Yu, *Energy Environ. Sci.*, 2022, **15**, 4647–4658.
210 Z. Cai, J. Liang, Z. Li, T. Yan, C. Yang, S. Sun, M. Yue, X. Liu, T. Xie, Y. Wang, T. Li, Y. Luo, D. Zheng, Q. Liu, J. Zhao, X. Sun and B. Tang, *Nat. Commun.*, 2024, **15**, 6624.
211 H. Hu, Z. Zhang, L. Liu, X. Che, J. Wang, Y. Zhu, J. P. Attfield and M. Yang, *Sci. Adv.*, 2024, **10**, eadn7012.
212 S. Bishwanathan and P. K. Gupta, *ACS Appl. Energy Mater.*, 2024, **7**, 5467–5478.
213 H. Mao, X. Liu, T. Cui, J. Tang, Z. Su, J. Chi, Y. Chai, Z. Wu and L. Wang, *Angew. Chem., Int. Ed.*, 2025, **64**, e202511867.
214 W. Xu, Z. Wang, P. Liu, X. Tang, S. Zhang, H. Chen, Q. Yang, X. Chen, Z. Tian, S. Dai, L. Chen and Z. Lu, *Adv. Mater.*, 2024, **36**, 2306062.
215 H. T. Dao, S. Sidra, V. H. Hoa, T. V. Tran, Q. H. Nguyen, P. K. L. Tran, M. Mai, S.-K. Kim, J. Kim and D. H. Kim, *Appl. Catal., B*, 2026, **386**, 126398.
216 K. Wan, T. Zhang, H. Wang, S. Liu, C. Xie, R. Gao, Y. Qin, X. Yang, Y. Guo, L. Wang and J. Liu, *Innov. Mater.*, 2025, **3**, 100148.
217 Z. Shi, Z. Niu, W. Guo, Y. Leng, Y. Chen, H. Li and J. Huang, *Adv. Mater.*, 2026, **38**, e13754.
218 H. Chen, R. Ding, Z.-W. Zeng, X.-X. Jia, Y.-C. Zhang, B.-W. Liu, F.-R. Zeng, Y.-Z. Wang and H.-B. Zhao, *Adv. Funct. Mater.*, 2025, **35**, 2505802.
219 J. G. Vos, T. A. Wezendonk, A. W. Jeremiasse and M. T. M. Koper, *J. Am. Chem. Soc.*, 2018, **140**, 10270–10281.
220 D. A. Bushiri, A. F. Baxter, O. Odunjo, D. V. Fraga Alvarez, Y. Yuan, J. G. Chen and D. V. Esposito, *ACS Appl. Energy Mater.*, 2024, **7**, 5479–5489.
221 A. A. Bhardwaj, J. G. Vos, M. E. S. Beatty, A. F. Baxter, M. T. M. Koper, N. Y. Yip and D. V. Esposito, *ACS Catal.*, 2021, **11**, 1316–1330.
222 Z. Li, J. Liang, S. Hong, Y. Ren, M. Zhang, S. Sun, Z. Cai, C. Yang, H. Wang, Y. Luo, S. Liu, Y. Yao, F. Gong, X. Sun and B. Tang, *Nat. Commun.*, 2025, **16**, 10327.
223 P. Wang, P. Wang, T. Wu, X. Sun and Y. Zhang, *Adv. Sci.*, 2024, **11**, 2407892.

224 T. Binninger, R. Mohamed, K. Waltar, E. Fabbri, P. Levecque, R. Kötz and T. J. Schmidt, *Sci. Rep.*, 2015, **5**, 12167.
225 N. Akbari, J. H. Shah, C. Hu, S. Nandy, P. Aleshkevych, R. Ge, S. Farid, C. Dong, L. Zhang, K. H. Chae, W. Xie, T. Liu, J. Wang and M. M. Najafpour, *Angew. Chem.*, 2025, **137**, e202418798.
226 D. Wu, L. Hu, X. Liu, T. Liu, X. Zhu, Q. Luo, H. Zhang, L. Cao, J. Yang, Z. Jiang and T. Yao, *Nat. Commun.*, 2025, **16**, 726.
227 G. Li, Y. Li, J. Dong, B. Sun, Z. Liu, J. Zheng and G. Li, *Adv. Funct. Mater.*, 2026, **36**, e15680.
228 J. Fu, X. Kong, X. Liu, H. Ma, L. Guo, J. Chi, X. Liu and L. Wang, *Adv. Funct. Mater.*, 2025, **36**, e23937.
229 D. Y. Chung, P. P. Lopes, P. Farinazzo Bergamo Dias Martins, H. He, T. Kawaguchi, P. Zapol, H. You, D. Tripkovic, D. Strmcnik, Y. Zhu, S. Seifert, S. Lee, V. R. Stamenkovic and N. M. Markovic, *Nat. Energy*, 2020, **5**, 222–230.
230 Q. Sha, T. Gao, L. Yan, W.-H. Hung, C.-Y. Chiang, D. Zhou, B. Liu, Y. Kuang and X. Sun, *J. Am. Chem. Soc.*, 2025, **147**, 20716–20724.
231 H. Liu, W. Shen, H. Jin, J. Xu, P. Xi, J. Dong, Y. Zheng and S.-Z. Qiao, *Angew. Chem., Int. Ed.*, 2023, **62**, e202311674.
232 J.-T. Ren, L. Chen, H.-Y. Wang, W.-W. Tian and Z.-Y. Yuan, *Energy Environ. Sci.*, 2024, **17**, 49–113.
233 T. Wang, X. Cao and L. Jiao, *Angew. Chem., Int. Ed.*, 2022, **61**, e202213328.
234 D. Bao, L. Huang, Y. Zheng and S.-Z. Qiao, *ACS Catal.*, 2025, **15**, 14661–14670.
235 K. Liu, X. Gao, C.-X. Liu, R. Shi, E. C. M. Tse, F. Liu and Y. Chen, *Adv. Energy Mater.*, 2024, **14**, 2304065.
236 P. Wang, X. Gao, M. Zheng, M. Jaroniec, Y. Zheng and S.-Z. Qiao, *Nat. Commun.*, 2025, **16**, 2424.
237 N. Sarigul, F. Korkmaz and İ. Kurultak, *Sci. Rep.*, 2019, **9**, 20159.
238 X. Gao, S. Zhang, P. Wang, M. Jaroniec, Y. Zheng and S.-Z. Qiao, *Chem. Soc. Rev.*, 2024, **53**, 1552–1591.
239 X. Gao, J. Hu, S. Zhang, P. Wang, Z. Wang, P. Chen, Y. Zheng and S.-Z. Qiao, *Adv. Mater.*, 2025, **38**, e21945.
240 F. Sun, J. Qin, Z. Wang, M. Yu, X. Wu, X. Sun and J. Qiu, *Nat. Commun.*, 2021, **12**, 4182.
241 R. Ding, J. Chen, Y. Chen, J. Liu, Y. Bando and X. Wang, *Chem. Soc. Rev.*, 2024, **53**, 11390–11461.
242 M. Clapp, C. M. Zalitis and M. Ryan, *Catal. Today*, 2023, **420**, 114140.
243 S. Shiva Kumar and V. Himabindu, *Mater. Sci. Energy Technol.*, 2019, **2**, 442–454.
244 A. Villagra and P. Millet, *Int. J. Hydrogen Energy*, 2019, **44**, 9708–9717.
245 M. Ni, M. K. H. Leung and D. Y. C. Leung, *Energy Convers. Manage.*, 2008, **49**, 2748–2756.
246 G. Chen, R. Lu, Z. Zhuang, H. Fei, X. Li, X. Zhang, C. Ma, J. Weng, J. Wang, J. Shang, T. Gan, Y. Wang, Z. Wang and Y. Han, *Sci. Adv.*, 2025, **11**, eaea4543.
247 J. Li, S. Fu, R. Wang, K. Sun, W. Shi, Y. Zeng and B. Zhang, *Nat. Commun.*, 2025, **16**, 9910.
248 A. S. Emam, M. O. Hamdan, B. A. Abu-Nabah and E. Elnajjar, *Int. J. Hydrogen Energy*, 2024, **64**, 599–625.
249 Q. Zhang, Y. Hao, H. Chen, J. Li, Y. Zeng, J. Xiong, Y. Cheng, A. Ozden, A. Tricoli and F. Li, *Adv. Energy Mater.*, 2026, **16**, e04039.
250 M. Schalenbach, W. Lueke and D. Stolten, *J. Electrochem. Soc.*, 2016, **163**, F1480–F1488.
251 Q. Li, A. Molina Villarino, C. R. Peltier, A. J. Macbeth, Y. Yang, M.-J. Kim, Z. Shi, M. R. Krumov, C. Lei, G. G. Rodríguez-Calero, J. Soto, S.-H. Yu, P. F. Mutolo, L. Xiao, L. Zhuang, D. A. Muller, G. W. Coates, P. Zelenay and H. D. Abruña, *J. Phys. Chem. C*, 2023, **127**, 7901–7912.
252 S. Dresp, F. Dionigi, S. Loos, J. Ferreira de Araujo, C. Spöri, M. Gliech, H. Dau and P. Strasser, *Adv. Energy Mater.*, 2018, **8**, 1800338.
253 G. Prats Vergel, H. Mu, N. Kolobov, J. Biemolt, D. A. Vermaas and T. Burdyny, *Nat. Chem. Eng.*, 2025, **2**, 676–684.
254 S. Z. Oener, M. J. Foster and S. W. Boettcher, *Science*, 2020, **369**, 1099–1103.
255 M. A. Blommaert, D. Aili, R. A. Tufa, Q. Li, W. A. Smith and D. A. Vermaas, *ACS Energy Lett.*, 2021, **6**, 2539–2548.
256 L. Bi, S. Boulfrad and E. Traversa, *Chem. Soc. Rev.*, 2014, **43**, 8255–8270.
257 Y. Zheng, J. Wang, B. Yu, W. Zhang, J. Chen, J. Qiao and J. Zhang, *Chem. Soc. Rev.*, 2017, **46**, 1427–1463.
258 A. Hauch, R. Küngas, P. Blennow, A. B. Hansen, J. B. Hansen, B. V. Mathiesen and M. B. Mogensen, *Science*, 2020, **370**, eaba6118.
259 C. K. Lim, Q. Liu, J. Zhou, Q. Sun and S. H. Chan, *J. Power Sources*, 2017, **342**, 79–87.
260 R. Rossi, D. M. Hall, L. Shi, N. R. Cross, C. A. Gorski, M. A. Hickner and B. E. Logan, *Energy Environ. Sci.*, 2021, **14**, 6041–6049.
261 J. Tang, K. Guo, D. Guan, Y. Hao and Z. Shao, *Energy Environ. Sci.*, 2024, **17**, 7394–7402.
262 H. Xie, Z. Zhao, T. Liu, Y. Wu, C. Lan, W. Jiang, L. Zhu, Y. Wang, D. Yang and Z. Shao, *Nature*, 2022, **612**, 673–678.
263 X. Liu, J. Chi, Y. Zhao, R. Huang, H. Zhang, J. Fu, Z. Ren, Y. Han, T. Wei, W. Song, H. Yu and Z. Shao, *Adv. Energy Mater.*, 2025, **15**, e03388.
264 M. L. Frisch, T. N. Thanh, A. Arinchtein, L. Hager, J. Schmidt, S. Brückner, J. Kerres and P. Strasser, *ACS Energy Lett.*, 2023, **8**, 2387–2394.
265 H. Liu, Y. Yang, J. Liu, M. Huang, K. Lao, Y. Pan, X. Wang, T. Hu, L. Wen, S. Xu, S. Li, X. Fang, W.-F. Lin, N. Zheng and H. B. Tao, *ACS Appl. Mater. Interfaces*, 2024, **16**, 16408–16417.
266 Y. Feng, Y. Zhu, W. Chen, X. Huang, X. Weng, M. D. Meyer, T.-H. Chen, Y. Liu, Z. He, C.-H. Hou, K. Zuo, N. Y. Yip, K. Gong, J. Lou and Q. Li, *Nat. Commun.*, 2025, **16**, 8618.
267 F.-Y. Gao, J. Xu, H. Shen, J.-W. DuanMu, M. Jaroniec, Y. Zheng and S.-Z. Qiao, *Nat. Commun.*, 2025, **16**, 11625.
268 L. Zhang, Z. Wang and J. Qiu, *Adv. Mater.*, 2022, **34**, 2109321.
269 H. Shi, T. Wang, J. Liu, W. Chen, S. Li, J. Liang, S. Liu, X. Liu, Z. Cai, C. Wang, D. Su, Y. Huang, L. Elbaz and Q. Li, *Nat. Commun.*, 2023, **14**, 3934.

270 Y. Lai, K. Xiao, Y. Tian, M. Xing, H. Ding, J. Tan, J. Zhang, Z. Peng, Y. Fan, X. Lu, S. Liang, W. Xue and X. Huang, *Nat. Sustainability*, 2026, **9**, 533–543.
271 W. Tang, Z. Zhao, D. Yang, Y. Liu, L. Zhu, Y. Wu, C. Lan, W. Jiang, Y. Wu, T. Liu and H. Xie, *Energy Environ. Sci.*, 2025, **18**, 7048–7059.
272 A. Bar, O. Ramon, Y. Cohen and S. Mizrahi, *J. Food Eng.*, 2002, **55**, 193–199.
273 S. Xu, Z. Zhou, Z. Liu and P. Sharma, *Sci. Adv.*, 2023, **9**, eade3240.
274 W. Li, P. N. Lemougna, K. Wang, Y. He, Z. Tong and X. Cui, *Ceram. Int.*, 2017, **43**, 14340–14346.
275 X. Gao, P. Wang, X. Sun, M. Jaroniec, Y. Zheng and S.-Z. Qiao, *Angew. Chem., Int. Ed.*, 2025, **64**, e202417987.
276 J. T. Davis, J. Qi, X. Fan, J. C. Bui and D. V. Esposito, *Int. J. Hydrogen Energy*, 2018, **43**, 1224–1238.
277 S. M. H. Hashemi, M. A. Modestino and D. Psaltis, *Energy Environ. Sci.*, 2015, **8**, 2003–2009.
278 M. I. Gillespie, F. van der Merwe and R. J. Kriek, *J. Power Sources*, 2015, **293**, 228–235.
279 E. A. Toledo-Carrillo, M. García-Rodríguez, L. M. Sánchez-Moren and J. Dutta, *Sci. Adv.*, 2024, **10**, eadi3180.
280 X. Yan, J. Biemolt, K. Zhao, Y. Zhao, X. Cao, Y. Yang, X. Wu, G. Rothenberg and N. Yan, *Nat. Commun.*, 2021, **12**, 4143.
281 A. Song, S. Mei, X. Jin, Y. Ma and J. Yang, *Angew. Chem., Int. Ed.*, 2025, **64**, e19128.
282 G. Ruan, F. Todman, G. Yogev, R. Arad, T. Smolinka, J. O. Jensen, M. D. Symes and A. Rothschild, *Nat. Rev. Clean Technol.*, 2025, **1**, 380–395.
283 I. Slobodkin, E. Davydova, M. Sananis, A. Breytus and A. Rothschild, *Nat. Mater.*, 2024, **23**, 398–405.
284 P. J. McHugh, A. D. Stergiou and M. D. Symes, *Adv. Energy Mater.*, 2020, **10**, 2002453.
285 Z. P. Ifkovits, J. M. Evans, M. C. Meier, K. M. Papadantonakis and N. S. Lewis, *Energy Environ. Sci.*, 2021, **14**, 4740–4759.
286 R. Cui, Z. Zhang, Y. Wang, F. Liu, H. Wang, C. Bi, C. Yu and Y. Zhou, *Int. J. Hydrogen Energy*, 2024, **50**, 635–649.
287 J. M. Allwood, *Nat. Chem. Eng.*, 2026, **3**, 26–33.
288 L. Gao, C. Wang, L. Yang, X. Huo, W. Li and J. Zhang, *Chem. Eng. J.*, 2025, **520**, 165784.
289 R. Mahmud, S. M. Moni, K. High and M. Carbajales-Dale, *J. Cleaner Prod.*, 2021, **317**, 128247.
290 M. Yong, M. Tang, L. Sun, F. Xiong, L. Xie, G. Zeng, X. Ren, K. Wang, Y. Cheng, Z. Li, E. Li, X. Zhang and H. Wang, *Nat. Sustainability*, 2024, **7**, 1662–1671.
291 X. Wang, H. Hu, J. Liu, J. Hu, C. Han, J. P. Attfield and M. Yang, *Adv. Mater.*, 2025, **37**, e08705.
292 J.-C. J. Kalinski, A. K. Pakkir Mohamed Shah, B. Ruiz Brandão Da Costa, S. P. Farrell, L. Schellenberg, L. G. Graves, T. Schramm, P. Stincone, I. Koester, B. M. Stephens, R. R. Torres, L. Cancelada, C. Utermann-Thüsing, Z. A. Quinlan, L. Wegley Kelly, C. A. Carlson, C. Castillo-Ilabaca, S. Pantoja-Gutiérrez, J. M. Beman, A. Hartmann, A. Aron, X. Siwe Noundou, R. A. Dorrington, D. Tasdemir, A. F. Haas, P. C. Dorrestein, C. E. Nelson, L. I. Aluwihare, M. Wang and D. Petras, *Nat. Geosci.*, 2026, **19**, 478–487.
293 X.-M. Hu, H.-Q. Liang, A. Rosas-Hernández and K. Daasbjerg, *Chem. Soc. Rev.*, 2025, **54**, 1216–1250.
294 P. Aleta, A. Refaie, M. Afshari, A. Hassan and M. Rahimi, *Energy Environ. Sci.*, 2023, **16**, 4944–4967.